Supporting Information

Dalmanol biosyntheses require coupling of two separate polyketide gene clusters

Zhen Zhen Zhou,[a] Hong Jie Zhu,[a] Li Ping Lin,[bc] Xuan Zhang,[a] Hui Ming Ge,[a] Rui Hua Jiao,[a] and Ren Xiang Tan*[ab]

[a]State Key Laboratory of Pharmaceutical Biotechnology, Institute of Functional Biomolecules, Nanjing University, Nanjing 210023, China.

[b]State Key Laboratory Cultivation Base for TCM Quality and Efficacy, Nanjing University of Chinese Medicine, Nanjing 210023, China.

[c]State Key Laboratory Elemento-organic Chemistry, Nankai University, Tianjin 300071, China.

*Corresponding authors: rxtan@nju.edu.cn

Table of Contents

Experimental Procedures

Strains and culture conditions

D. eschscholzii was grown on potato dextrose agar (PDA) for 4 days at 28 °C. The fresh mycelia were inoculated into 400 mL malt extract (ME) medium (20 g/L malt extract, 20 g/L sucrose and 1 g/L peptone) in 1000 mL flasks for 10 days at 28 °C, 140 rpm. For the fermentation of *TF1 OE* strain, maltose monohydrate was added to ME medium up to 1% (w/v) to activate the α-amylase (*amyB*) promoter.

A. oryzae NSAR1 (*niaD*$^{-}$, *sC*$^{-}$, Δ*argB*, *adeA*$^{-}$) was used as the host for heterologous expressions. Transformants of the *A. oryzae* strain were cultivated in 400 mL DPY medium (20 g/L dextrin, 10 g/L polypeptone, 5 g/L yeast extract, 5 g/L KH_2PO_4 and 0.5 g/L $MgSO_4 \cdot 7H_2O$) in 1000 mL baffled flasks for 1 day at 28 °C, 140 rpm. The fresh cells were inoculated (1:10) into 400 mL CDS medium (3 g/L $NaNO_3$, 1 g/L $KH_2PO_4 \cdot 3H_2O$, 0.5 g/L $MgSO_4 \cdot 7H_2O$, 0.01 g/L $FeSO_4 \cdot 7H_2O$, 0.55 g/L $CaCl_2$, 2 g/L starch and 1 g/L polypeptone) in 1000 mL baffled flasks, and shaken for further 2 days at 28 °C, 140 rpm. Maltose monohydrate was added to CDS medium up to 2% (w/v) to activate the α-amylase (*amyB*) promoter.

E. coli DH5α was used as a host for molecular cloning. The *E. coli* cells carrying certain plasmid were grown in Luria-Bertani (LB) medium with appropriate antibiotics at 37 °C, 200 rpm.

Bioinformatic analysis of PKS domains

Modular analysis of PKSs in *D. eschscholzii* was performed by using the antiSMASH (fungal version). The boundaries of MT domains were identified using Conserved Domain Database (CCD) of the National Center for Biotechnology (NCBI) program. Protein sequences of NR-PKSs from other fungi were also obtained from the NCBI database.

RNA preparation and real-time quantitative PCR (qPCR) analysis of expression of *PKS* genes

D. eschscholzii was cultured in ME medium for 48 h at 30°C, 140 rpm. The fresh mycelia were harvested by filtration and ground under liquid nitrogen. Total RNA was extracted using TRIzol reagent (Invitrogen) according to the manufacturer's instructions. After treated with DNase I (Takara), the total RNA was reverse transcribed using the first strand cDNA synthesis Kit (Thermo Fisher Scientific). A qPCR assay was performed to validate the expression level of each *PKS* gene using SYBR Green master mix (Roche) according to the manufacturer's instructions. Gene expression levels were calculated using the $2^{-\Delta\Delta Ct}$ method. Beta tubulin gene was used as an internal control. The primers used for amplifying the target genes are listed in Table S1†.

Construction of deletion or overexpression mutants of *D. eschscholzii*

Homologous recombination based on split-marker strategy was used to delete the entire gene. For single-deletions of *ChrA* and *ChrB*, fusion PCR was performed to generate DNA–deletion cassette containing hygromycin-resistance marker (hygromycin phosphotransferase gene, *Hph*) with *trpC* promoter and *trpC* terminator.[1] For the *4HNR* and *TF1* deletion, the gene-deletion cassette was generated by homologous recombination using a ClonExpress II One Step Cloning Kit (Vazyme Biotech). About 1.5 kb of 5' and 3' flanking sequences were PCR amplified from the genomic DNA of *D. eschscholzii*. Split *Hph* was PCR amplified from plasmid pSH75. *D. eschscholzii* was inoculated for 36

hours at 30°C and 140 rpm in a 200 mL growth medium containing 1% yeast extract, 1% casamino acid, and 2% sucrose. The harvested hyphae were digested with 30 mg/mL lysing enzyme (Sigma-Aldrich, L1412) and 10 mg/mL driselase (Sigma-Aldrich, D9515) to produce the protoplasts. Transformation of gene deletion cassettes was accomplished by PEG-mediated transformation of protoplast. Diagnostic PCR was performed to identify mutant strains with hygromycin B (200 μg/mL) resistance.

For the *TF1* overexpression, the native promoter of *TF1* was replaced by *AmyB* promoter through transforming an overexpression cassette containing *Hph* gene.

For the double-deletion of *ChrA* and *4HNR*, *ChrA*-deletion cassette containing *Bar* gene was transformed to the *4HNR*-deleted mutant strain, and glufosinate-ammonium (4 mg/mL) was used for the selection of transformants.

Construction of fungal expression plasmids

The full-length sequence of each gene was amplified from the *D. eschscholzii* genomic DNA, with the primers listed in Table S1†. After purification, *pksTL*, *4HNR*, *ChrA*, and *ChrB* were ligated into the pTAex3, pUSA or pAdeA vector by homologous recombination using a ClonExpress II One Step Cloning Kit (Vazyme Biotech). Both pTAex3 and pUSA were digested by KpnI to get linearlized vectors used for the in-fusion cloning. For pAdeA, XbaI was used to get a linearlized vector.

For constructing mutant *ChrA* with point mutations in ketoreductase (KR) domain, pTAex3-*ChrA* was used as the template, overlap PCR was performed to generate site mutation DNA fragments that ligated to pTAex3 vector by in-fusion cloning. Each of the *ChrA* mutants (*ChrA*-M1, *ChrA*-M2, and *ChrA*-M3) was co-expressed with *ChrB*, with all mutants and *ChrB* containing *AmyB* promoter and terminator ligated to pTAex3.

Transformation of *A. oryzae* NSAR1

A. oryzae was inoculated in 200 mL DPY medium for 12 hours at 30°C and 140 rpm. The harvested hyphae were digested with 20 mg/mL lysing enzyme and 5 mg/mL driselase to produce the protoplasts. Transformation of *A. oryzae* was also performed by the PEG-mediated transformation. To co-express *pksTL* and *4HNR*, pUSA-*4HNR* was further transformed to the pTAex3-*pksTL* transformant. Similarly, the pTAex3-*ChrA* transformant was further transformed with pUSA-*ChrB* to construct the *ChrA* and *ChrB* co-expressing strain. The *ChrA*/*ChrB*-AO co-transformant was transformed with pAdeA-*pksTL* to construct the *pksTL*/*ChrA*/*ChrB*-AO co-expressing strain (Table S5†).

The *ChrA*-M1-AO, *ChrA*-M2-AO, and *ChrA*-M3-AO transformants were transformed with pTAex3-*ChrA*-M1, pTAex3-*ChrA*-M2, and pTAex3-*ChrA*-M3, respectively. The *ChrA*-M1/ChrB-AO, *ChrA*-M2/ChrB-AO, and *ChrA*-M3/ChrB-AO co-transformants were transformed with pTAex3-*ChrA*-M1+*ChrB,* pTAex3-*ChrA*-M2+*ChrB*, and pTAex3-*ChrA*-M3+*ChrB*, respectively.

LC-HR/MS analysis of metabolites

The crude extracts derived from the cultures of *D. eschscholzii* and *A. oryzae* were analyzed by LC-HR/MS at the following conditions: a linear gradient from 20% to 70% CH_3CN for 25 min, 100% CH_3CN for 3 min, and 20% CH_3CN for 2 min (flow rate: 0.5 mL/min). Solvents were: A, HPLC grade H_2O with 0.1% TFA; B, HPLC grade CH_3CN.

For feeding experiments of *ChrB-AO*, the LC-HR/MS conditions were: a linear gradient from 30% to 100% CH_3CN for 18 min, and kept at 100% CH_3CN for 2 min (flow rate: 0.5 mL/min).

HPLC analysis of metabolites in *A. oryzae*

The crude extracts derived from the cultures of *A. oryzae* were analyzed by HPLC at the following conditions: a linear gradient from 10% to 70% CH_3CN for 25 min, 100% CH_3CN for 3 min, and 10% CH_3CN for 2 min (flow rate: 0.5 mL/min). Solvents were: A, HPLC grade H_2O with 0.1% TFA; B, HPLC grade CH_3CN.

Feeding experiments of *ChrB*-AO

For feeding experiments in *A. oryzae*, **9** and **10** (1 mg each) were separately added to 100 mL of CDS medium with 2% maltose monohydrate at the time of inoculation of the *ChrB*-AO transformant. After further incubation at 28 °C for 2 days, the fermentation broth was extracted with ethyl acetate twice and concentrated *in vacuo*. Such dried extracts were dissolved in methanol for the LC-HR/MS analysis.

Chemical complementation assays in the *D. eschscholzii* mutants

Compounds **3** or **4** (1 mg each) were added to 400 mL culture of the Δ*ChrA*/Δ*4HNR* strain at 48 h after inoculation. 4HN (10 mg) was added to 400 mL culture of the Δ*pksTL* strain at 48 h after inoculation. After further incubation at 28 °C for 8 days, the fermentation broth was extracted with ethyl acetate twice and concentrated *in vacuo*. Such dried extracts were dissolved in methanol for the LC-HR/MS analysis.

Monooxygenase inhibition assays

Monooxygenase inhibitors (specified below) were separately added to fungal culture at 48 h after inoculation. The concentration of each inhibitor was 1 mM (for FMO inhibitor, methimazole) or 0.1 mM (for P450 inhibitors, phenylbutazone and proadifen). After further incubation at 28 °C for 8 days, the fermentation broth was extracted with ethyl acetate twice and concentrated *in vacuo*. Such dried extracts were dissolved in methanol for the HPLC analysis.

Metabolite purification procedure

Purification of 3 and 4

The extract (34 g) derived from the culture of the *ChrA*/*ChrB*-AO co-transformant was subjected to silica-gel column chromatography and eluted stepwise using a petroleum ether/acetone gradient (100:0 → 50:50). Fractions containing **3** were further purified by reverse-phase preparative HPLC (55% aqueous methanol, 2.0 mL/min) to yield 2.3 mg of **3** as white amorphous solid; ^1H and ^{13}C NMR data, assigned and listed in Table S6†; HR/ESIMS: *m/z* 195.0653 $[M+H]^+$ (calcd for $C_{10}H_{11}O_4$, 195.0652). Fractions that contained **4** were further purified by reverse-phase preparative HPLC (35% aqueous CH_3CN, 2.0 mL/min) to yield 1.6 mg of **4** as yellow brown amorphous solid; ^1H and ^{13}C NMR spectral assignment is tabulated (Table S7†); HR/ESIMS: *m/z* 179.0706 $[M+H]^+$ (calcd for $C_{10}H_{11}O_3$, 179.0708). Compound **15** (5.0 mg, yellowish solid) was obtained by reverse-phase preparative HPLC (CH_3CN/H_2O, 35%). ^1H and ^{13}C NMR spectral assignment is tabulated (Table S8†); HR/ESIMS: *m/z* 323.0564 $[M+Na]^+$ (calcd for $C_{13}H_{16}O_6SNa$, 323.0560).

Purification of 9 and 10

The extract (26 g) derived from the culture of the *ChrA*-AO transformant was subjected to silica-gel column chromatography and eluted stepwise using a petroleum ether/acetone gradient (100:0 → 50:50). Fractions containing **9** were further purified by reverse-phase preparative HPLC (70% aqueous methanol, 2.0 mL/min) to yield 8.1 mg of **9** as white powder: ^{1}H NMR (600 MHz, acetone-d_6) δ: 0.96 (3H, t, J = 7.2 Hz, CH_3), 1.68 (2H, sextet, J = 7.2 Hz, H-2), 3.06 (2H, t, J = 7.2 Hz, H-2), 5.94 (2H, s, H-6, H-8), 9.18 (1H, br s, 7-OH), 11.7 (1H, s, 5-OH). HR/ESIMS: *m/z* 197.0811 $[M+H]^+$ (calcd for $C_{10}H_{13}O_4$, 197.0808). These spectral data are identical with those of **9** acquired upon its first-time isolation.[2] The fractions containing **10** were further purified by reverse-phase preparative HPLC (65% aqueous methanol, 2.0 mL/min) to give 48.6 mg of **10** as colorless needles: ^{1}H NMR (400 MHz, acetone-d_6) δ: 1.47 (3H, d, J = 6.4 Hz, CH_3), 2.63 (1H, dd, J = 17.2 and 3.2 Hz, H-3a), 2.69 (1H, dd, J = 17.2 and 12.4 Hz, H-3b), 4.60 (1H, dqd, J = 12.4, 6.4, and 3.2 Hz, H-2), 5.93 (2H, s, H-6, H-8), 9.62 (1H, br s, 7-OH), 12.2 (1H, s, 5-OH). HR/ESIMS: *m/z* 195.0651 $[M+H]^+$ (calcd for $C_{10}H_{11}O_4$, 195.0652). These data are identical with those recorded for **10** upon its first-time characterization.[3]

Purification of 20a and 20b

The extract (70 g) derived from the culture of *TF1 OE* was further separated via RP-18 column washed with gradient aqueous MeOH (10% → 100%) to yield 7 fractions (Frs. 1–7). Fr. 3 was submitted to Sephadex LH-20 (MeOH) followed by reverse-phase preparative HPLC (CH_3CN/H_2O, 31%) to produce **20a** {1.0 mg, yellow solid, HR/ESIMS *m/z* 335.0911 $[M+H]^+$ (calcd for $C_{20}H_{15}O_5$, 335.0914)} and **20b** {1.3 mg, yellow solid, HR/ESIMS *m/z* 333.0754 $[M+H]^+$ (calcd for $C_{20}H_{13}O_5$, 333.0757)}. ^{1}H and ^{13}C NMR data, see Table S9†.

Purification of 13 and 14

The extract (10 g) derived from the culture of *ChrA*-M2/*ChrB*-AO co-transformant was subjected to silica-gel column chromatography and eluted stepwise using a petroleum ether/acetone gradient (100:0 → 50:50). Fractions containing **13** and **14** were further purified by reverse-phase preparative HPLC (21% CH_3CN/H_2O, 2.0 mL/min) to yield **13** {8 mg, white solid, HR/ESIMS *m/z* 211.0604 $[M+H]^+$ (calcd for $C_{10}H_{11}O_5$, 211.0601)} and **14** {12.8 mg, brown solid, HR/ESIMS *m/z* 169.0494 $[M+H]^+$ (calcd for $C_8H_9O_4$, 169.0495)}. ^{1}H and ^{13}C NMR data of **13** was assigned and listed in (Table S6†). These data of **14** are identical with those recorded upon its previous characterization.[4]

Supplementary Tables

Table S1 Primers used in this study

Primer	Sequence (5'–3')	Purpose
ChrA-1F	GAGACGGCGGCTAACATG	*ChrA* deletion
ChrA-1R	gctccttcaatatcatcttctgGAAGACGGTGATTCAAAGTAAGG	
hph-1F	CAGAAGATGATATTGAAGGAGC	Gene deletion
hph-1R	GCGGATTCCTCAGTCTCG	
hph-2F	ACCTGCCTGAAACCGAAC	Gene deletion
hph-2R	GGATCCTCTAGAAAGAAGGATTAC	
ChrA-2F	gtaatccttctttctagaggatccCCAGGGTCTCAAGCAACG	*ChrA* deletion
ChrA-2R	CACCGAGGATGCGAAGGA	
Diag-ChrA-F	CCAAACAGACATAGCCAAGG	Verification of Δ*ChrA*
Diag-ChrA-R	CTCGGGCATCTCAAATACAG	
ChrB-1F	TCGGACCACCTTCACCTCA	*ChrB* deletion
ChrB-1R	tccttcaatatcatcttctgACATCTATCTGGCCTAAGT	
ChrB-2F	tccttctttctagaggatccTCATACGAGCGATTGCTCG	*ChrB* deletion
ChrB-2R	CGATTATTGTCTACGCTGTC	
Diag-ChrB-F	ATGAAGTGCCTTACCGATGC	Verification of Δ*ChrB*
Diag-ChrB-R	TTACTTTGGCGCTTTCCTG	
InF-4HNR-1F	cggggatcctctagagtcgacATCCCTTCACCTTTGCCAC	*4HNR* deletion
InF-4HNR-1R	tccttcaatatcatcttctgTTGAGAAATGGATTTATGCACC	
InF-4HNR-2F	tccttctttctagaggatccTTTGCACAGGCCAAGTCA	*4HNR* deletion
InF-4HNR-2R	cttgcatgcctgcaggtcgacATTGCCACTTGTAGGTCTGC	
Diag-4HNR-F	GGTCTTCCAAATCCCTTCA	Verification of Δ*4HNR*
Diag-4HNR-R	GGTTACTCATAGCGGTGGG	
Diag-pksTL-F	AACATCGTCGCTAATGCTTG	Verification of Δ*pksTL*
Diag-pksTL-R	AGCCTTTCCCGCCCATAGT	
lacTL-P1	AATGCTGGAGACGCTTTGTT	Verification of Δ*lacTL*
lacTL-P2	ACAATCCCGCAGGACCAT	
lacTL-P3	CATTCCAGTCGTATGTCACCG	
lacTL-P4	GTCTCGGGCACTAACACCAT	
lacTL-P5	GCGGATTCCTCAGTCTCG	
lacTL-P6	ACCTGCCTGAAACCGAAC	
InF-ChrA-AO-F	ttcgagctcggtaccATGAGTCAACCAACTGGACG	*ChrA* expression in *A. oryzae*
InF-ChrA-AO-R	agatccccgggtaccTTAACCTTCCAATAATCGTTGC	
InF-ChrB-AO-F	ttcgagctcggtaccATGACTCGAGTACTTCTAACTGGC	*ChrB* expression in *A. oryzae*
InF- ChrB-AO-R	agatccccgggtaccTTACAATAGACCCTTGATACTCTCC	
InF-pksTL-AO-F	ttcgagctcggtaccATGGCGGACCAGATGGCTT	*pksTL* expression in *A. oryzae*
InF- pksTL-AO-R	agatccccgggtaccTTAGCGGTGGATACCGTCCT	
InF-4HNR-AO-F	ttcgagctcggtaccATGCCTTCCGCCGGCCCA	*4HNR* expression in *A. oryzae*
InF-4HNR-AO-R	agatccccgggtaccCTAAGTGCCACCACCCGAAG	
2009-qPCR-F	TCCGTCACGCACCTCATTC	qPCR
2009-qPCR-R	AGCATACGCTCGCAACCC	
2828-qPCR-F	TGACTGTTCTGTCGCTATTGCTG	qPCR
2828-qPCR-R	TGTGCCAGAGGCTTGAGGA	
pksTL-qPCR-F	CGGCCGATCTCTTAGGTCAC	qPCR
pksTL-qPCR-R	CCTTGAAGCAGGACGGATGT	
6333-qPCR-F	ACACCGTCTTCAACGATCCC	qPCR
6333-qPCR-R	GGTGGATATCGCGCTCTGAA	
ChrA-qPCR-F	TTCGACGCTGGTCTCTTCAC	qPCR
ChrA-qPCR-R	GTTACACCGGCACTCTCCAA	
8186-qPCR-F	TAGCAGGCGTCATCAAAGCA	qPCR
8186-qPCR-R	ATGGCTTAGCCTGGGCATTT	

9039-qPCR-F	GACAGCCAACAGCCGAACC	qPCR
9039-qPCR-R	GCATTCAGCAGGGAGACCAG	
9576-qPCR-F	GTGGAGCGTCAGAAACAAGC	qPCR
9576-qPCR-R	CACTTCGCATTCATAAGCCAC	
ChrB-qPCR-F	AGGCGAGGAGTATCCCGAGTA	qPCR
ChrB-qPCR-R	CCACTACACCCACGACGGAT	
TuB-qPCR-F	GACACCGTCGTTGAGCCTTAC	Reference gene for qPCR
TuB-qPCR-R	ACCAGGGAAACGCAAGCA	
Inf-ChrA-M1-1R	GGCACCTTCGACGTCGGGCGAGAGACCCTCAAC	*ChrA*-M1 expression in *A. oryzae*
ChrA-M1-2F	GACGTCGAAGGTGCCTGGAAC	
Inf-ChrA-M2-1R	GGTTGCGACGATGGCACTGGTGACGACGAAGAAGT	*ChrA*-M2 expression in *A. oryzae*
ChrA-M2-2F	GCCATCGTCGCAACCATCAAC	
Inf-ChrA-M3-1R	GTTGGCGGCGTTGGCGTTAGCCTGGCCGGGAAC	*ChrA*-M3 expression in *A. oryzae*
ChrA-M3-2F	GCCAACGCCGCCAACACTTTC	

Table S2 NR- and PR-PKSs in *D. eschscholzii*

Gene no.	Architecture of PKS module	Type
2009	SAT-KS-AT-PT-ACP-ACP-R	NR-PKS
2828	SAT-KS-AT-DH-ACP-MT-Aes	NR-PKS
5781 (*pksTL*)	SAT-KS-AT-PT-ACP-ACP-TE	NR-PKS
6333	KS-AT-DH-SDR-KR-ACP	PR-PKS
8183 (*ChrA*)	KS-AT-DH-MT-KR-ACP	PR-PKS
8186	KS-AT-DH-MT-KR-ACP	PR-PKS
9576	SAT-KS-AT-PT-ACP-MT-R	NR-PKS

Aes: Acetyl esterase/lipase

Table S3 The chromane gene cluster in *D. eschscholzii* and deduced gene function

gene	Amino acids	Predicted function	Protein homologue, origin	Protein coverage (%)	Similarity/ Identity (%)
orf1	610	Developmental regulatory protein	WetA (I1S0E2), *Fusarium graminearum* PH-1	97	40/28
orf2	470	Hypothetical protein	XP_011315610, *Fusarium graminearum* PH-1	97	48/31
orf3	456	Probable transporter	ApdF (Q5ATG7) , *Aspergillus nidulans* FGSC A4	91	57/37
orf4, ChrB	340	Ketoreductase	CgKR1 (5B6K_A), *Candida Glabrata*	98	54/37
orf5, *Chr*A	2089	Polyketide synthase	LovF (Q9Y7D5) , *Aspergillus terreus*	92	49/31
orf6	315	Hypothetical protein	XP_001910878, *Podospora anserina*	90	41/28

orf7	465	Glycerol uptake/efflux facilitator protein	Glpf (1LDF_A), *Escherichia coli*	50	46/30

Table S4 The naphthalene gene cluster in *D. eschscholzii* and deduced gene function

gene	Amino acids	Predicted function	Protein homologue, origin	Protein coverage (%)	Similarity/ Identity (%)
orf1	646	Beta-galactosidase	BgaC (4MAD_A), *Bacillus circulans*	91	54/38
orf2	113	isomerase	WP_057292910, *Noviherbaspirillum* sp. Root189	67	48/32
orf3	829	Transcription factor	XP_009216426, *Gaeumannomyces tritici* R3-111a-1	98	79/68
orf4, 4HNR	203	4HN reductase	4HNR (1JA9_A), *Magnaporthe grisea*	99	80/69
orf5	422	Transcription factor	TcpZ (TCPZ_CLAP2), *Claviceps purpurea*	89	37/23
orf6	117	-	-	-	-
orf7, pksTL	2161	Polyketide synthase	PKS1 (BAA18956), *Colletotrichum lagenaria*	99	81/70
orf8, lacTL	552	Laccase/Multicopper Oxidase	Fet3p (1ZPU_A), *Saccharomyces cerevisiae*	91	51/37
orf9	1486	RNA polymerase III	Pol III (5FJ8_A), *Saccharomyces cerevisiae*	96	70/55
ofr10	1031	Lipase and DDHD domain-containing protein	P87109, *Schizosaccharomyces pombe*	82	43/30

Table S5 *A. oryzae* strains used in this study

Genotype	Description
AO	*Aspergillus oryzae* auxotrophic mutant strain NSAR1 (*niaD*−, *sC*−, Δ*argB*, *adeA*−)
ChrA-AO	NSAR1 + pTAex3-*ChrA*
ChrB-AO	NSAR1 + pUSA-*ChrB*
ChrA/*ChrB*-AO	NSAR1 + pTAex3-*ChrA* + pUSA-*ChrB*
pksTL-AO	NSAR1 + pTAex3-*pksTL*
pksTL/*4HNR*-AO	NSAR1 + pTAex3-*pksTL* + pUSA-*4HNR*
pksTL/*ChrA*/*ChrB*-AO	NSAR1 + pTAex3-*ChrA* + pUSA-*ChrB* + pAdeA-*pksTL*
ChrA-M1-AO	NSAR1 + pTAex3-*ChrA*-M1
ChrA-M2-AO	NSAR1 + pTAex3-*ChrA*-M2
ChrA-M3-AO	NSAR1 + pTAex3-*ChrA*-M3
ChrA-M1/*ChrB*-AO	NSAR1 + pTAex3-*ChrA*-M1+*ChrB*
ChrA-M2/*ChrB*-AO	NSAR1 + pTAex3-*ChrA*-M2+*ChrB*
ChrA-M3/*ChrB*-AO	NSAR1 + pTAex3-*ChrA*-M3+*ChrB*

Table S6 ^{1}H (400 MHz) and ^{13}C NMR (100 MHz) data of **3** and **13**

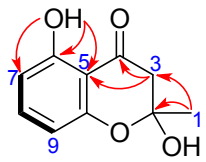

3

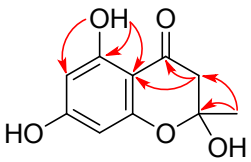

13

(Key HMBC, red arrows; ^{1}H-^{1}H COSY, bold lines)

Position	**3**		**13**	
	δ_C [a]	δ_H [a] (mult, *J*, Hz)	δ_C [b]	δ_H [b] (mult, *J*, Hz)
1	28.6	1.75 (s)	27.4	1.68 (s)
2	100.7		101.0	
3	47.1	2.97 (d, 17.0)	46.9	3.03 (d, 16.8)
		2.94 (d, 17.0)		2.73 (d, 16.8)
4	196.6		195.8	
5	107.6		102.0	
6	161.7		163.9	
7	109.9	6.53 (d, 8.4)	95.6	5.92 (d, 2.2)
8	138.3	7.37 (t, 8.4)	166.3	
9	107.8	6.41 (d, 8.4)	95.6	5.89 (d, 2.2)
10	158.1		160.8	
6-OH		11.56 (s)		12.09 (s)
8-OH				9.61 (s)

[a] in $CDCl_3$, [b] in acetone-d_6

Table S7 ^{1}H (600 MHz) and ^{13}C NMR (125 MHz) data of **4** (acetone-d_6)

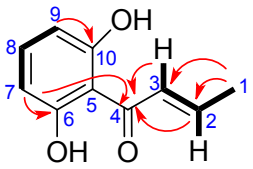

(Key HMBC, red arrows; ^{1}H-^{1}H COSY, bold lines)

Position	δ_C	δ_H (mult, *J*, Hz)
1	17.7	1.95 (dd, 7.0, 1.2)
2	143.3	7.09 (dq, 14.6, 7.0)
3	132.0	7.53 (br d, 14.6)
4	194.6	
5	110.2	
6	162.0	
6-OH		11.46 (s)
7	107.5	6.43 (d, 7.8)
8	136.0	7.25 (t, 7.8)
9	107.6	6.43 (d, 7.8)
10	162.0	
10-OH		11.46 (s)

Table S8 ^{1}H (400 MHz) and ^{13}C NMR (100 MHz) data **15** (acetone-d_6)

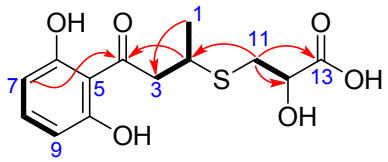

15

(Key HMBC, red arrows; ^{1}H-^{1}H COSY, bold lines)

Position	δ_C	δ_H (mult, J, Hz)
1	21.1	1.33 (d, 6.7)
2	36.1	3.61 (overlap)
3	52.1	3.58 (overlap) 3.26 (dd, 18.4, 9.5)
4	205.3	
5	110.2	
6	162.0	
7	107.6	6.45 (d, 8.2)
8	136.2	7.28 (t, 8.2)
9	107.6	6.45 (d, 8.2)
10	162.0	
11	34.7	3.04 (dd, 13.9, 4.4) 2.93 (dd, 13.9, 6.2)
12	70.7	4.39 (dd, 6.2, 4.4)
13	173.3	

Table S9 ^{1}H (600 MHz) and ^{13}C NMR (150 MHz) data **20a** and **20b** (DMSO-d_6)

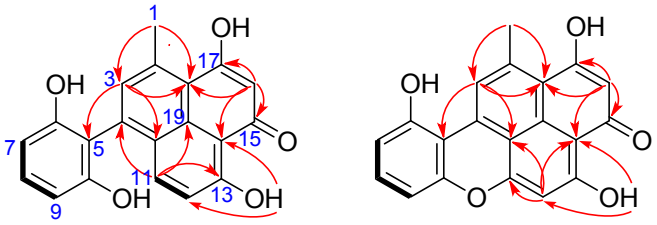

20a **20b**

(Key HMBC, red arrows; ^{1}H-^{1}H COSY, bold lines)

Position	**20a**		**20b**	
	δ_C	δ_H (mult, J, Hz)	δ_C	δ_H (mult, J, Hz)
1	25.4	2.93 (s)	26.1	3.01 (s)
2	143.5		146.0	
3	131.8	7.29 (s)	123.4	8.88 (s)
4	141.7		132.1	
5	113.4		106.7	
6	156.4		157.7	
7	106.9	6.48 (d, 8.2)	111.9	6.93 (d, 8.1)
8	129.9	7.08 (t, 8.2)	131.7	7.40 (t, 8.1)
9	106.9	6.48 (d, 8.2)	107.7	6.95 (d, 8.1)
10	156.4		152.4	
11	138.6	7.75 (d, 9.3)	157.9	
12	120.8	7.05 (d, 9.3)	100.2	6.62 (s)
13	174.5		176.7	
14	108.0		104.9	
15	181.6		177.5	
16	103.5	6.43 (s)	103.4	6.41 (s)
17	169.8		167.2	
18	118.1		116.0	
19	128.8		127.3	
20	123.4		110.9	
6-OH		9.29 (s)		
10-OH		9.29 (s)		
13-OH		17.57 (s)		18.03 (s)

Table S10 Monooxygenase genes found in the *D. eschscholzii* genome

Cytochrome P450							
GME8	GME1534	GME2861	GME4093	GME5901	GME7274	GME8192	GME9573
GME38	GME1557	GME3118	GME4094	GME5918	GME7391	GME8233	GME9659
GME53	GME1795	GME3146	GME4216	GME5923	GME7488	GME8307	GME9775
GME668	GME1809	GME3161	GME4221	GME6161	GME7636	GME8318	GME9898
GME1047	GME1855	GME3203	GME4587	GME6195	GME7690	GME8607	GME9923
GME1099	GME1894	GME3311	GME4589	GME6264	GME7703	GME8609	GME10131
GME1163	GME2007	GME3407	GME4590	GME6338	GME7725	GME8776	GME10202
GME1187	GME2210	GME3425	GME4622	GME6363	GME7854	GME8838	GME10644
GME1188	GME2216	GME3459	GME4625	GME6367	GME7856	GME9043	GME10709
GME1275	GME2235	GME3573	GME4994	GME6532	GME7870	GME9066	GME10710
GME1331	GME2236	GME3576	GME5452	GME6892	GME7897	GME9075	GME10736
GME1335	GME2397	GME3577	GME5623	GME6936	GME7937	GME9258	GME10806
GME1430	GME2430	GME3652	GME5625	GME7128	GME7968	GME9460	GME10807
GME1434	GME2723	GME3696	GME5789	GME7133	GME8085	GME9491	GME10825
GME1459	GME2763	GME3873	GME5866	GME7137	GME8096	GME9499	
Flavin-containing monooxygenase (FMO)							
GME21	GME1361	GME2186	GME3040	GME4506	GME6169	GME7822	GME9577
GME108	GME1390	GME2234	GME3074	GME4722	GME6483	GME7949	GME9749
GME184	GME1465	GME2601	GME3330	GME4830	GME6484	GME8119	GME9925
GME683	GME1493	GME2765	GME3496	GME4831	GME6607	GME8244	GME10137
GME969	GME1537	GME2778	GME3879	GME4972	GME6627	GME8558	GME10514
GME1201	GME1677	GME2795	GME3915	GME5054	GME6859	GME8930	GME10543
GME1211	GME1679	GME2811	GME3926	GME5187	GME6891	GME9102	GME10616
GME1213	GME1813	GME2827	GME3931	GME5417	GME6933	GME9266	GME10643
GME1226	GME2134	GME2944	GME4218	GME5466	GME7207	GME9387	GME10821
GME1229	GME2154	GME3003	GME4223	GME6168	GME7438	GME9488	

Supplementary Figures

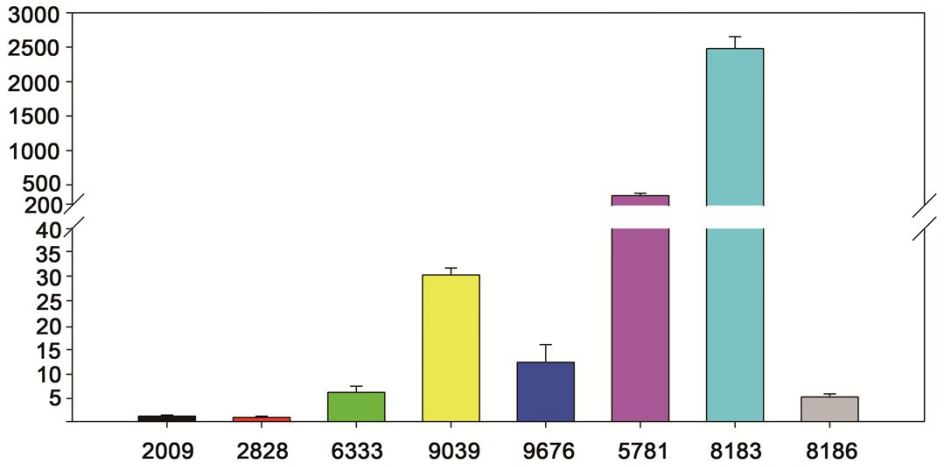

Fig. S1 qRT-PCR expression analysis of *NR*- and *PR-PKSs* in *D. eschscholzii*

The *PKS* expression levels were presented as relative expression fold ($2^{-\Delta\Delta Ct}$ values) to an *NR-PKS* (GME2009, 2009 for short). Error bars indicate the standard deviation (SD). The gene number of *pksTL* and *ChrA* was GME5781 (5781) and GME8183 (8183), respectively. Expression levels are individually normalized to expression of beta tubulin gene.

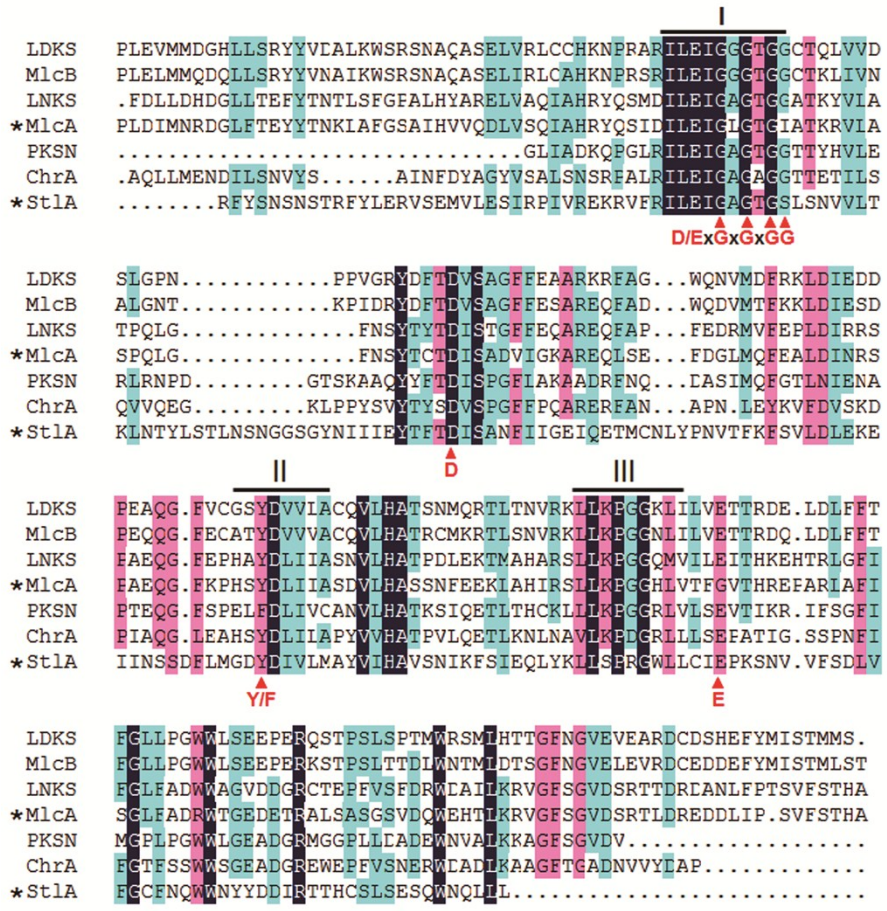

Fig. S2 Amino acid sequence alignment of MT domains of ChrA and other fungal PKSs

The amino acid sequence of ChrA-MT was aligned with both active and inactive PKS-MTs. Black line marks conserved motifs I, II, and III. The D/ExGxGxG residues of motif I involved in SAM binding are conserved in ChrA-MT. The putative key amino acids are shown in red and indicated by red arrows. Star (*) marks inactive PKS-MT.

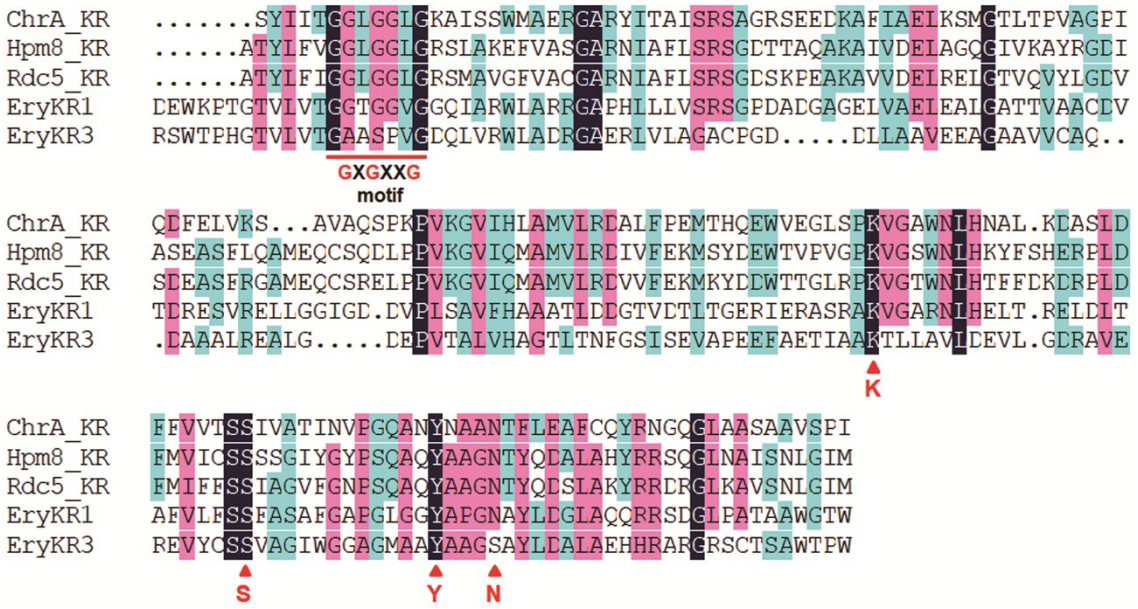

Fig. S3 Amino acid sequence alignment of KR domains of ChrA and other PKSs

The KR domain of Hpm8, Rdc5 and DEBS module 1 (EryKR1) were active, while that of DEBS module 3 (EryKR3) was inactive. The conserved sequence containing GXGXXG motif for NADPH binding is underlined. The catalytic residues K, S, Y and N are shown in red and indicated by red arrows.

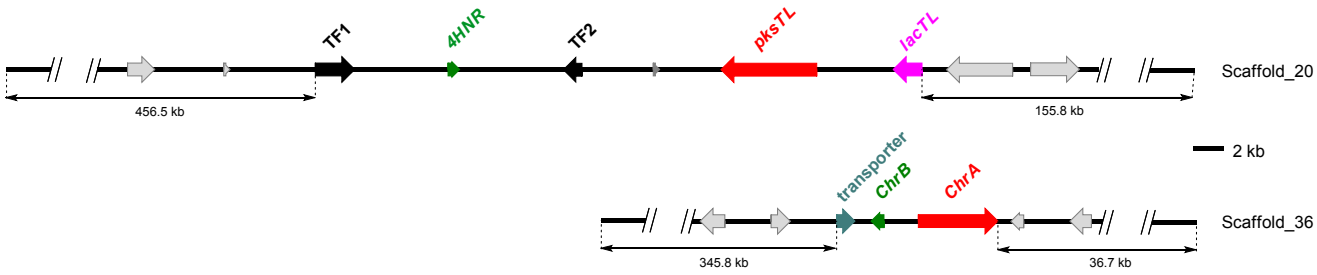

Fig. S4 The chromane and naphthalene gene clusters located apart on scaffolds 20 and 36

To evaluate the possibly short distance between the two clusters, the two scaffolds were supposed to anchor on the same chromosome. Thus, if scaffold 20 was upstreamed on scaffold 36, the inter-cluster distance should be 501 kb apart. On the contrary, the distance was 493 kb if scaffold 36 was at the upstream of scaffold 20.

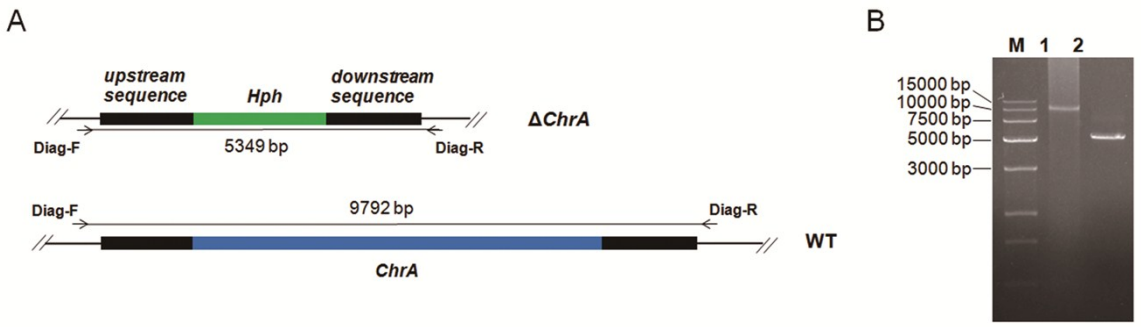

Fig. S5 Deletion of *ChrA* and PCR screening

(A) Schemes of the *ChrA* deletion using knock out cassette with *Hph* as a marker. (B) PCR amplification using diagnostic primers confirmed the genotype of the Δ*ChrA* mutant. The PCR products of the WT and mutant strains were displayed respectively in lanes 1 and 2, where primers Diag-F and Diag-R were used.

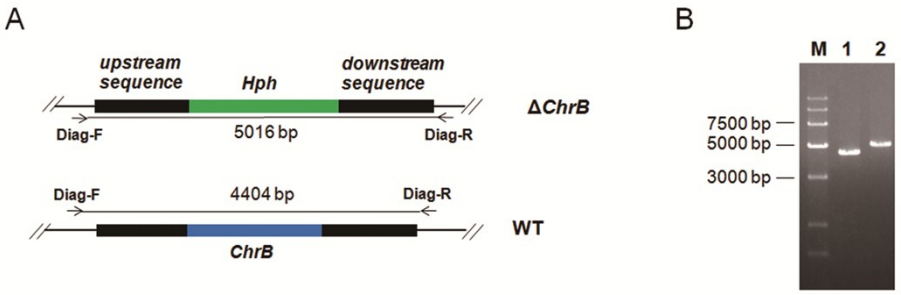

Fig. S6 Deletion of *ChrB* and PCR screening

(A) Schemes of the *ChrB* deletion using knock out cassette with *Hph* as a marker. (B) PCR amplification using diagnostic primers confirmed the genotype of the Δ*ChrB* mutant. The PCR products of the WT and mutant strains were respectively displayed in lanes 1 and 2, where primers Diag-F and Diag-R were used.

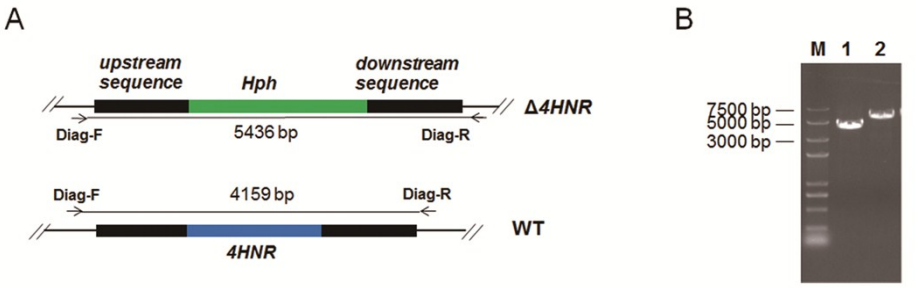

Fig. S7 Deletion of *4HNR* and PCR screening

(A) Schemes of the *4HNR* deletion using knock out cassette with *Hph* as a marker. (B) PCR amplification using diagnostic primers confirmed the genotype of the Δ*4HNR* mutant. The PCR products of the WT and mutant strains were displayed respectively in lanes 1 and 2, where primers Diag-F and Diag-R were used.

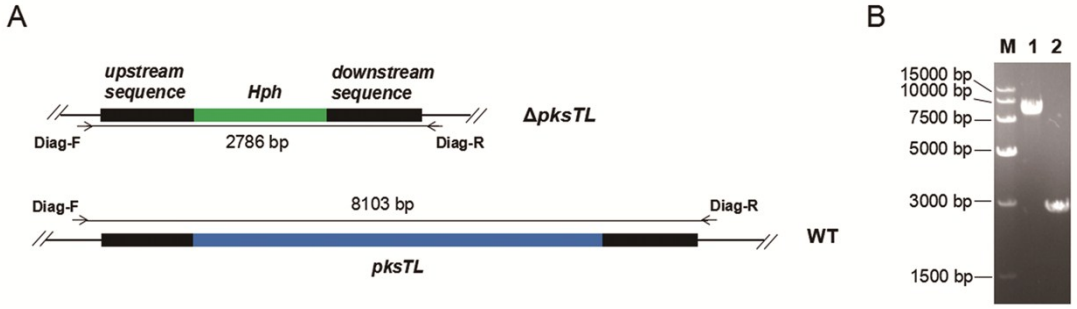

Fig. S8 Deletion of *pksTL* and PCR screening

(A) Schemes of the *pksTL* deletion using knock out cassette with *Hph* as a marker. (B) PCR amplification using diagnostic primers confirmed the genotype of the Δ*pksTL* mutant. The PCR products of the WT and mutant strains were displayed respectively in lanes 1 and 2, where primers Diag-F and Diag-R were used.

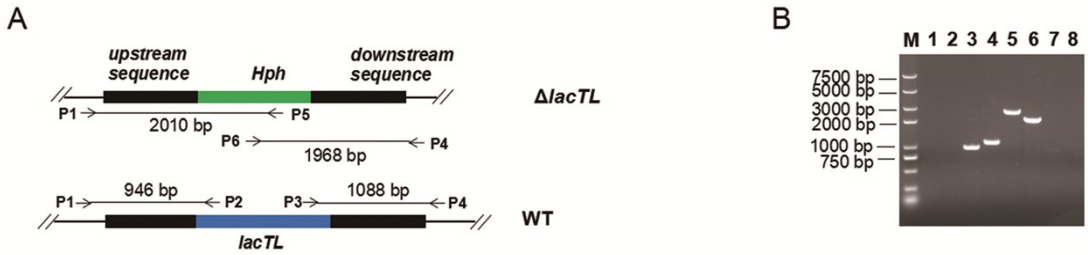

Fig. S9 Deletion of *lacTL* and PCR screening

(A) Schemes of the *lacTL* deletion using knock out cassette with *Hph* as a marker. (B) PCR amplification using diagnostic primers confirmed the genotype of the Δ*lacTL* mutant. Lane 1-4, PCR product of the WT strain; lane 5-6, PCR product of the mutant strain. Lane 1 and 5 used primers P1 and P5; lane 2 and 6 used primers P4 and P6; lane 3 and 7 used primers P1 and P2; lane 4 and 8 used primers P3 and P4.

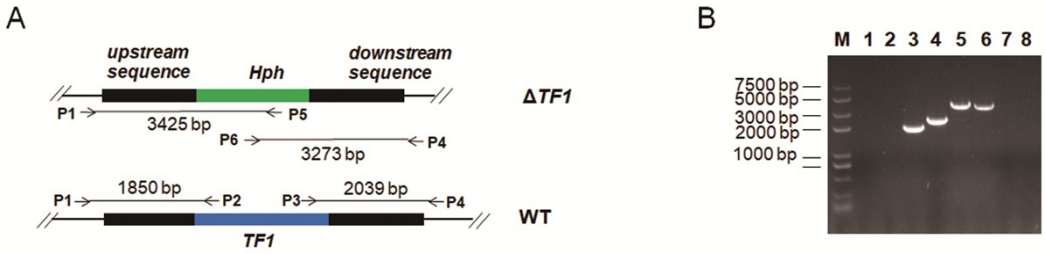

Fig. S10 Deletion of *TF1* and PCR screening

(A) Schemes of the *TF1* deletion using knock out cassette with *Hph* as a marker. (B) PCR amplification using diagnostic primers confirmed the genotype of the Δ*TF1* mutant. Lane 1-4, PCR product of the WT strain; lane 5-6, PCR product of the mutant strain. Lane 1 and 5 used primers P1 and P5; lane 2 and 6 used primers P4 and P6; lane 3 and 7 used primers P1 and P2; lane 4 and 8 used primers P3 and P4.

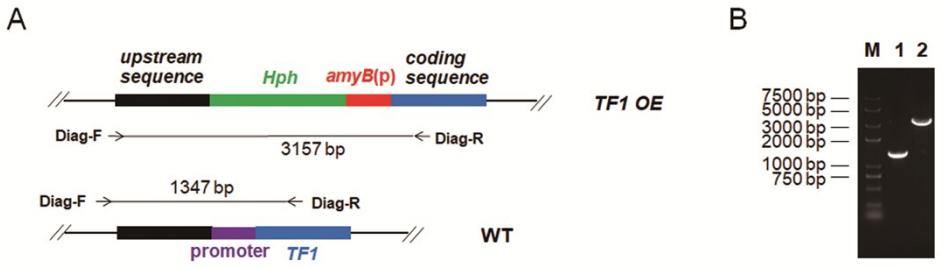

Fig. S11 Construction of *TF1* overexpression mutant and PCR screening

(A) Schemes of the *TF1* overexpression using promoter substitution cassette with *Hph* as a marker. (B) PCR amplification using diagnostic primers confirmed the genotype of the Δ*pksTL* mutant. The PCR products of the WT and mutant strains were displayed respectively in lanes 1 and 2, where primers Diag-F and Diag-R were used.

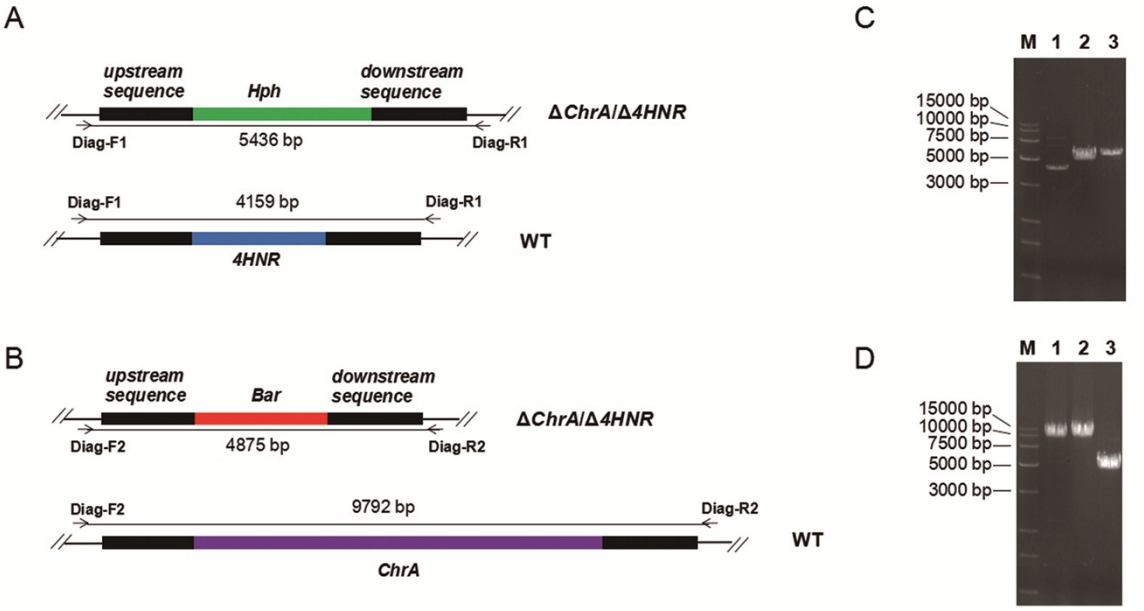

Fig. S12 Construction of Δ*ChrA*/Δ*4HNR* double mutant and PCR screening

(A) and (B) Schemes of the double-deletion of *4HNR* and *ChrA* using knock out cassette with *Hph* (for Δ*4HNR*) or *Bar* (for Δ*ChrA*) as a marker. (C) and (D) PCR amplification using diagnostic primers of Δ*4HNR* (C) or Δ*ChrA* (D) confirmed the genotype of the Δ*ChrA*/Δ*4HNR* mutant. The PCR products of the WT, Δ*4HNR*, and Δ*ChrA*/Δ*4HNR* strains were displayed respectively in lanes 1–3, where primers Diag-F and Diag-R were used.

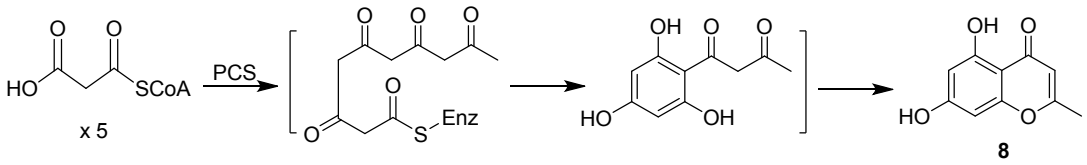

Fig. S13 The biosynthesis of **8** by a type III PKS

In *Rheum palmatum*, **8** is biosynthesized by a type III PKS (PCS) belonging to the chalcone synthase (CHS) superfamily.

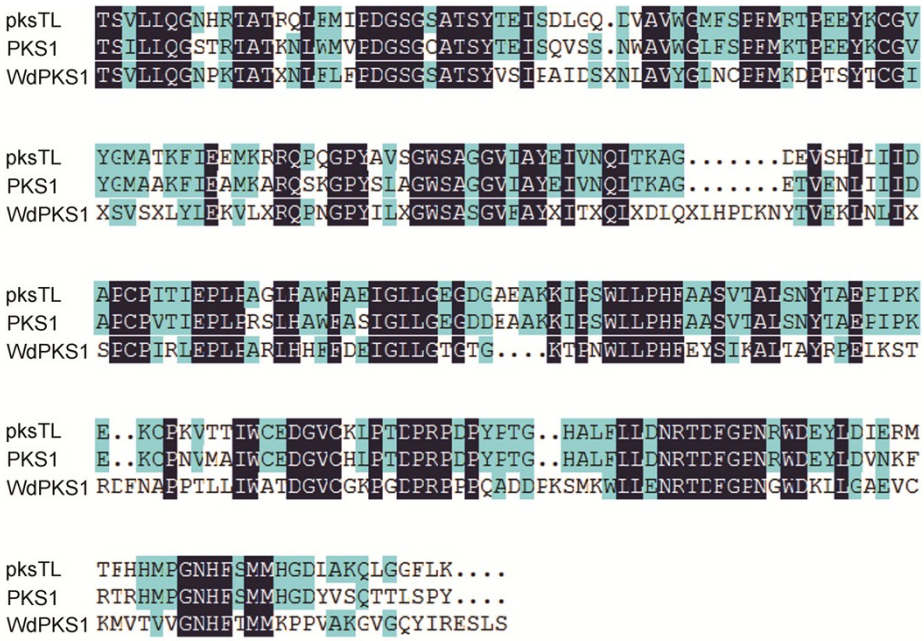

Fig. S14 Sequence alignment of TE domain of pksTL, PKS1, and WdPKS1

PKS1 and WdPKS1 catalyze the formation of 4HN and A4HN, respectively.

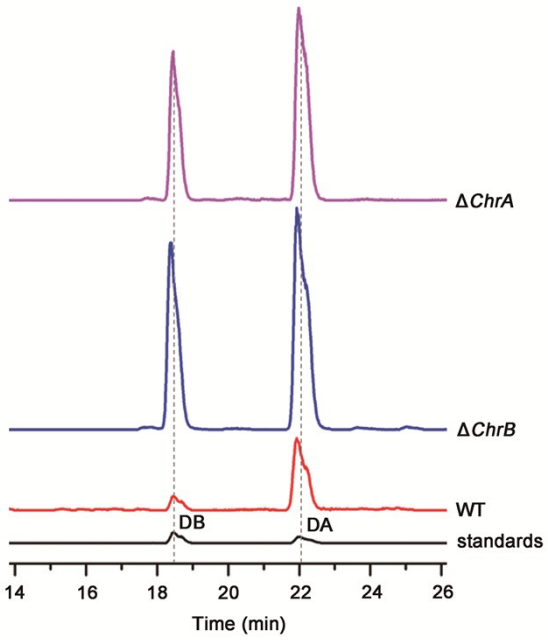

Fig. S15 Differentiated dalesconol productions among the Δ*ChrA,* Δ*ChrB*, and WT strains

LC-HR/MS screenings for dalesconols A (DA) and B (DB) among the Δ*ChrA,* Δ*ChrB*, and WT strains.

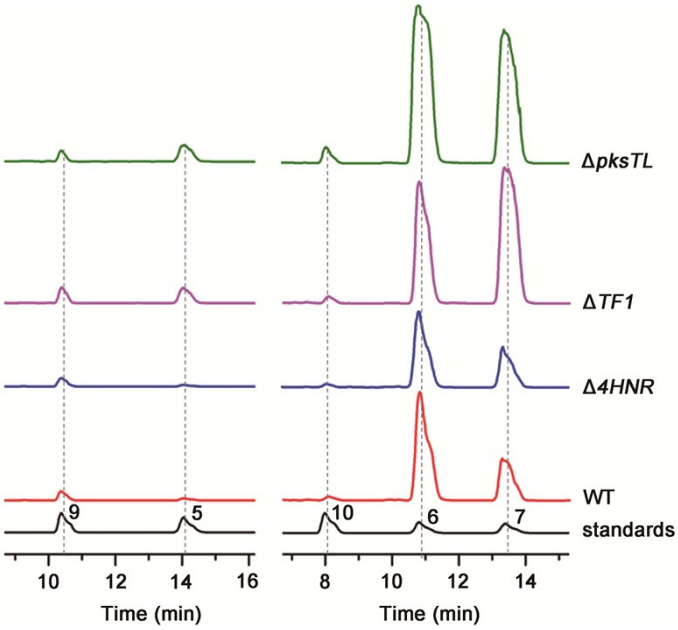

Fig. S16 Differentiated chromane pentaketide productions among the Δ*pksTL,* Δ*TF1,* Δ*4HNR*, and WT strains

LC-HR/MS screening for chromane pentaketides **5**–**7**, **9**, and **10** from the cultures of Δ*pksTL,* Δ*TF1,* Δ*4HNR* and WT strains.

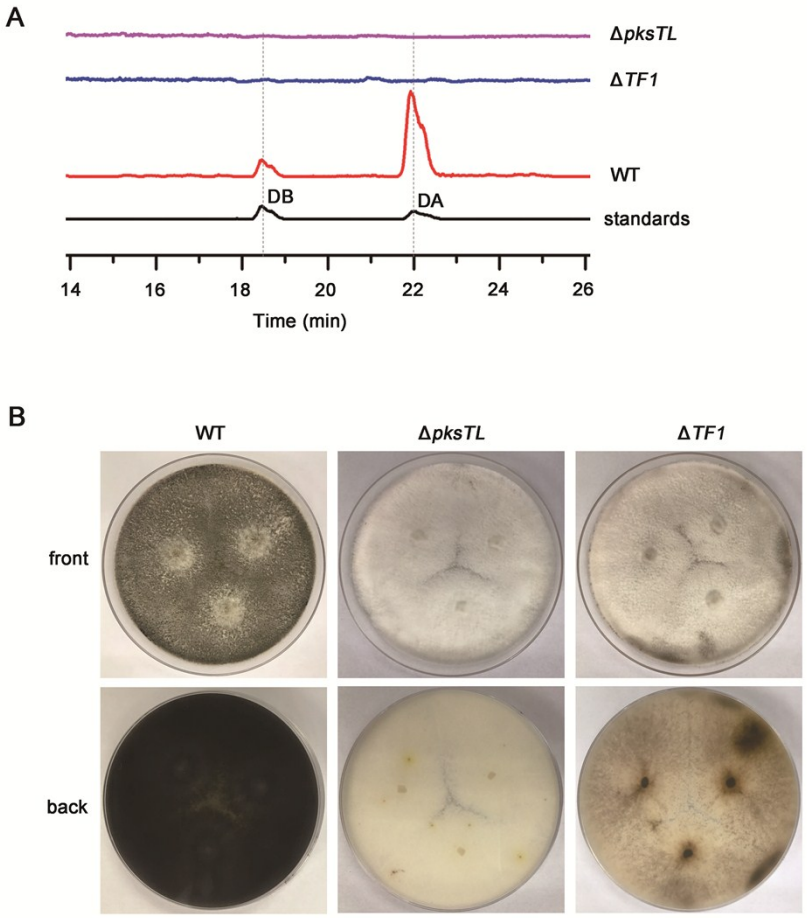

Fig. S17 The differentiated production of dalesconols and melanin among the Δ*pksTL,* Δ*TF1* and WT strains

(A) LC-HR/MS comparison of dalesconols A (DA) and B (DB) among the Δ*pksTL*, Δ*TF1* and WT strains. (B) Different strains were grown on PDA plates for 10 days. Both Δ*TF1* and Δ*pksTL* lost their ability to produce melanin.

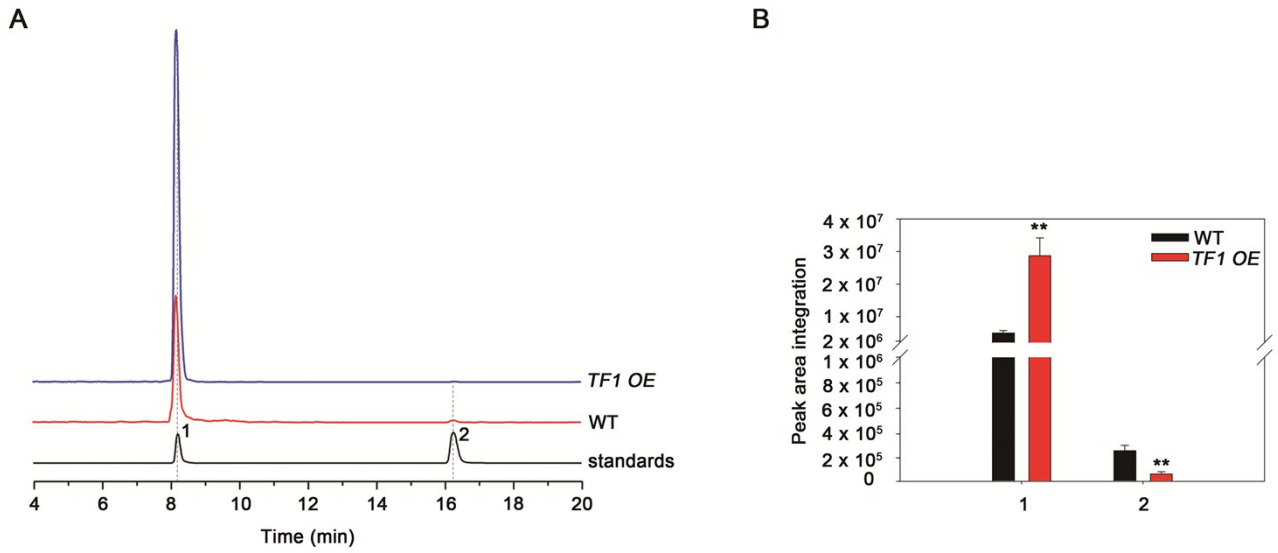

Fig. S18 LC-HR/MS comparison for the production of **1** and **2** between *TF1 OE* and WT strains.

The WT strain and mutants were compared through the LC-HR/MS profiling for the production of: (A) dalmanol A (**1**) and acetodalmanol A (**2**), with their peak areas integrated in (B). Data shown as mean ± SD (n = 3). ** indicated $P < 0.01$, by Student's *t* test.

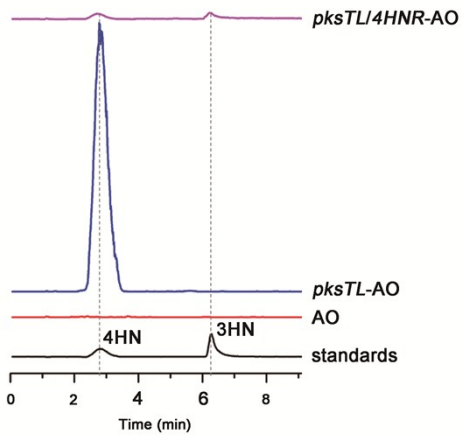

Fig. S19 Co-expression of *pksTL* and *4HNR* in *A. oryzae*

LC-HR/MS analyses of the extracts derived from the cultures of the *pksTL*-AO transformant and *pksTL/4HNR*-AO co-transformant, which produced an escalated level of 4HN only and a mixture of 4HN and 3HN, respectively.

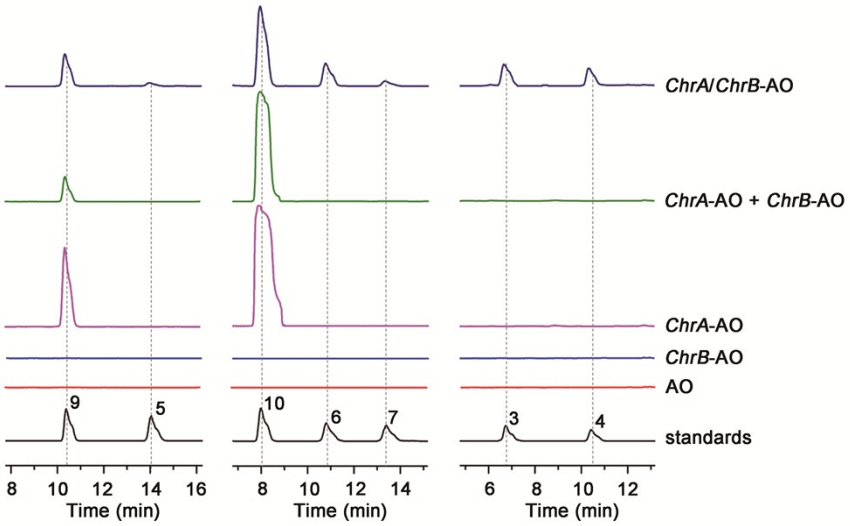

Fig. S20 Co-expression of *ChrA* and *ChrB* in *A. oryzae*

LC-HR/MS analyses of the extracts derived from the culture showed that the *ChrA*/*ChrB*-AO produced **5**–**7** along with the nascent intermediates **3** and **4**. Co-culture of *ChrA*-AO with *ChrB*-AO generated **9** and **10**, as did the culture of *ChrA*-AO alone.

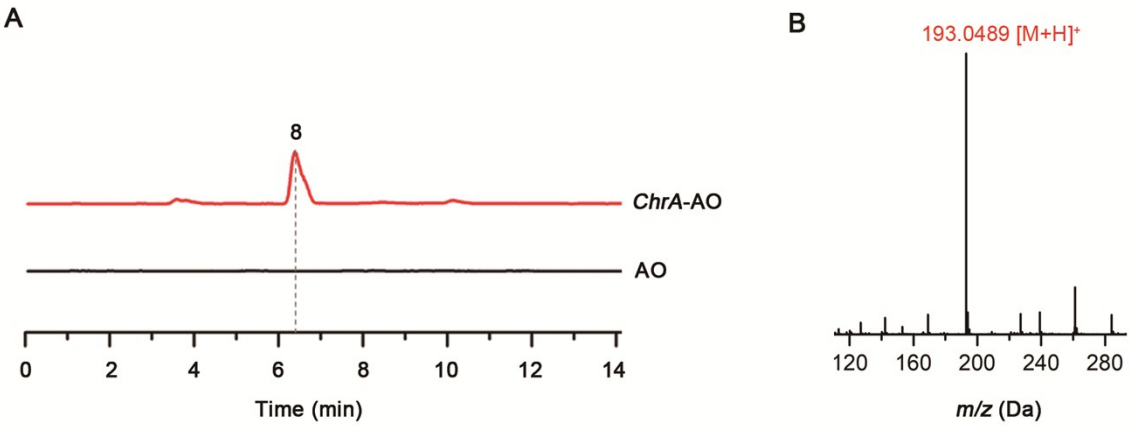

Fig. S21 LC-HR/MS detection of **8** in the *ChrA*-AO strain

EIC (A) and MS (B) profiles of **8** in *ChrA*-AO strain are shown.

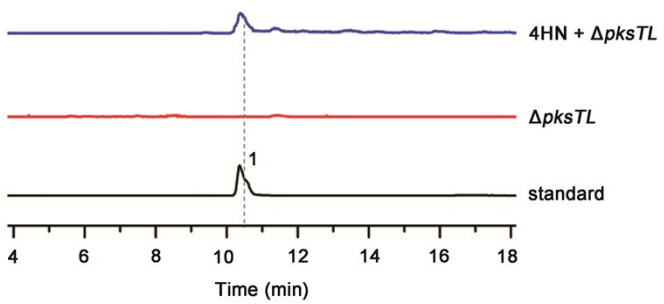

Fig. S22 Chemical complementation of 4HN in the Δ*pksTL* mutant

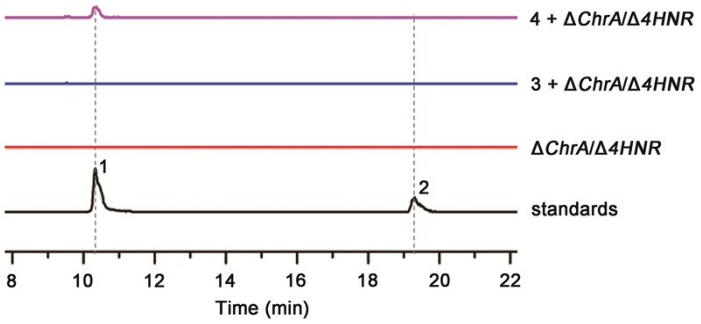

Fig. S23 Chemical complementation of **3** or **4** in the Δ*ChrA*/Δ*4HNR* mutant

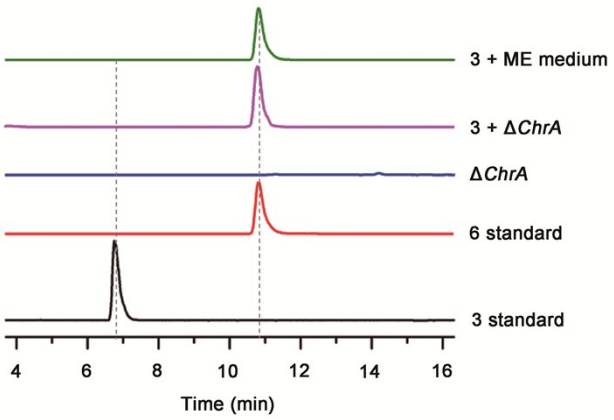

Fig. S24 Non-enzymatic conversion of **3** to **6**

Addition of **3** restored the production of **6** by the Δ*ChrA* mutant, but **3** was also converted to **6** in ME medium used for culturing *D. eschscholzii.*

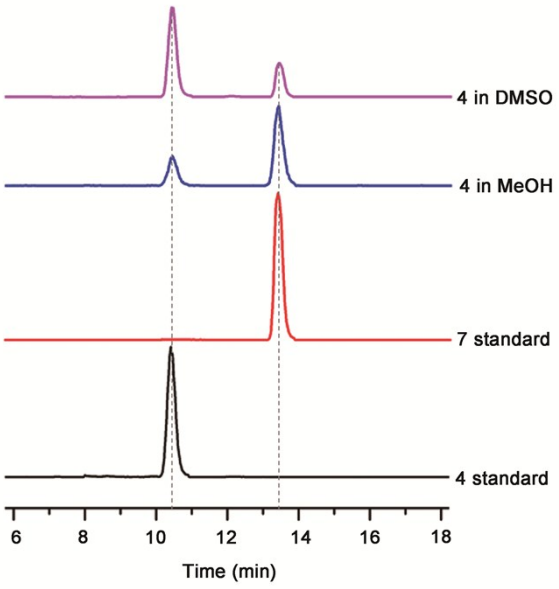

Fig. S25 Spontaneous conversion of **4** to **7** in MeOH and DMSO

In acetone, **4** was stable, but rapidly conversed to **7** after diluted with MeOH or DMSO as evidenced from the LC-HR/MS screening.

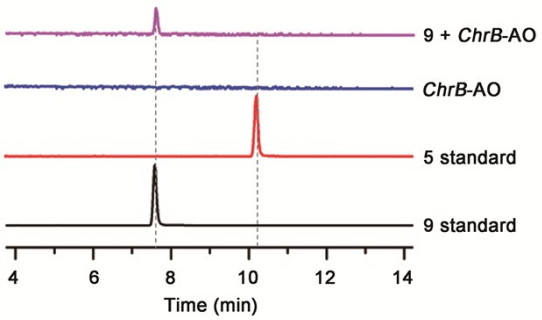

Fig. S26 No transformation of **9** into **5** by the *ChrB*-AO transformant

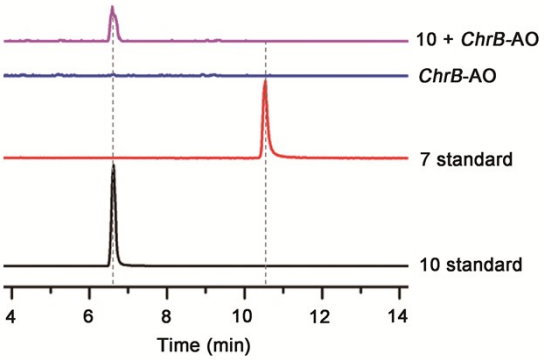

Fig. S27 No transformation of **10** to **7** by the *ChrB*-AO transformant

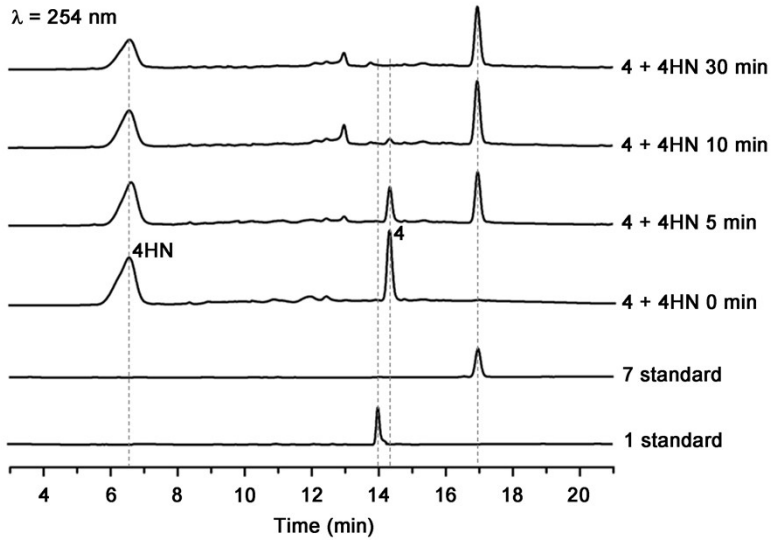

Fig. S28 PBEO (**4**) and 4HN were incubated together in the ME medium

HPLC profiling of the co-incubation products of 1mM PBEO (**4**) and 1mM 4HN in the ME medium used for culturing *D. eschscholzii* for 0, 5, 10 and 30 min at 30 °C.

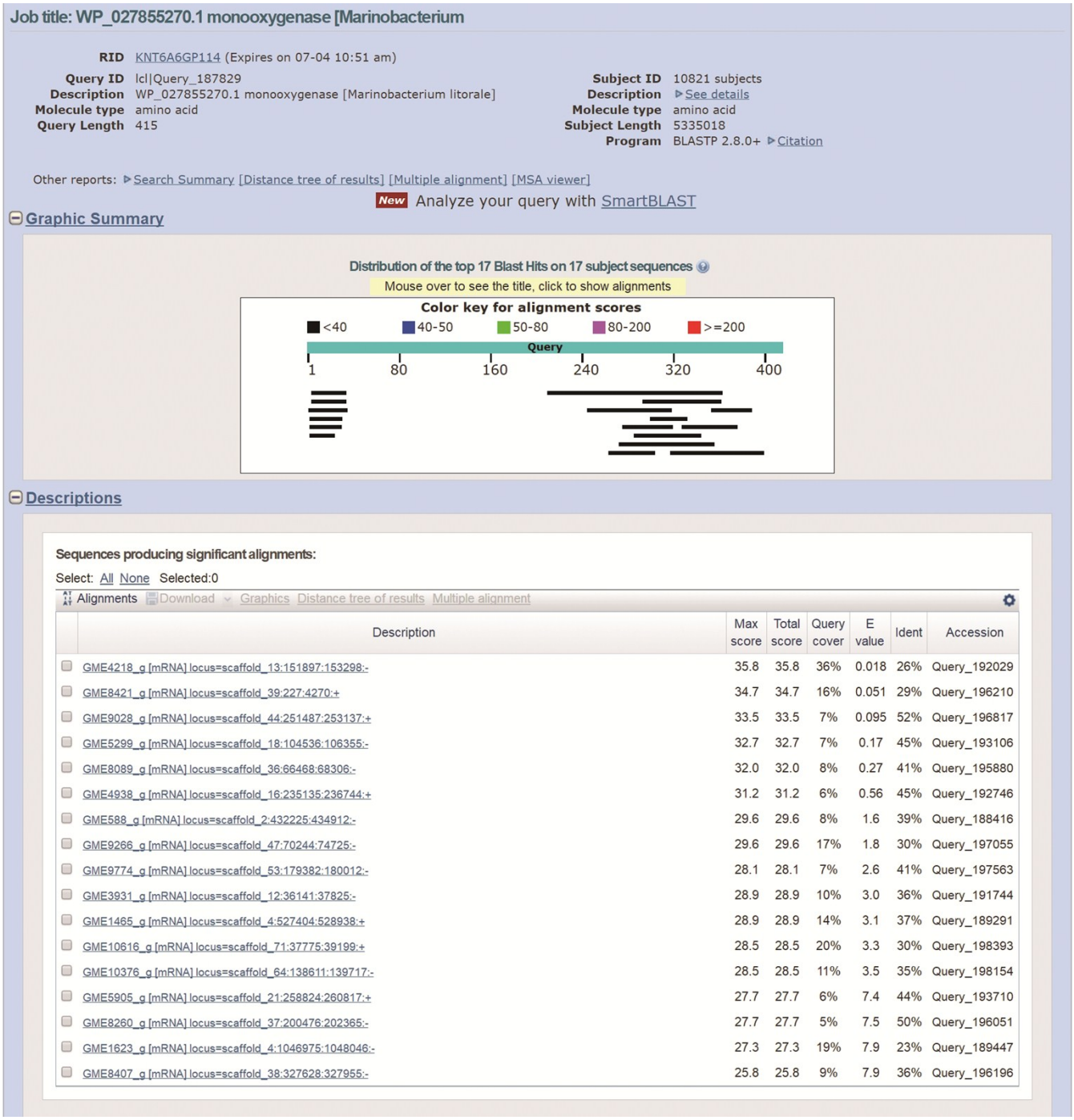

Fig. S29 Sequence blast result between styrene monooxygenase StyA and all proteins encoded by the *D. eschscholzii* genome

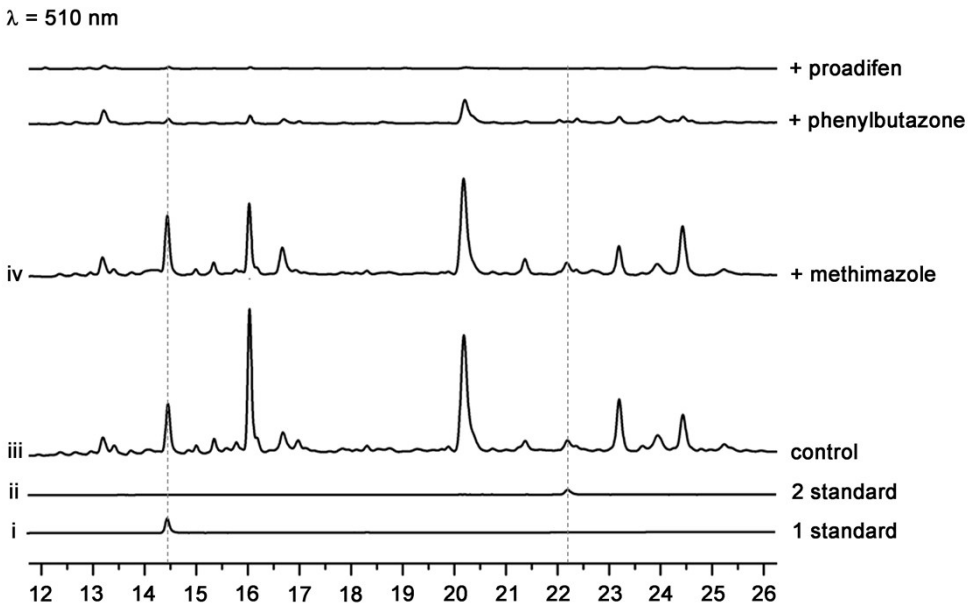

Fig. S30 HPLC comparison for the production of **1** and **2** in the *D. eschscholzii* cultures exposed separately to monooxygenase inhibitors including the FMO inhibitor methimazole (1 mM) and P450 inhibitors— phenylbutazone (0.1 mM) and proadifen (0.1 mM)

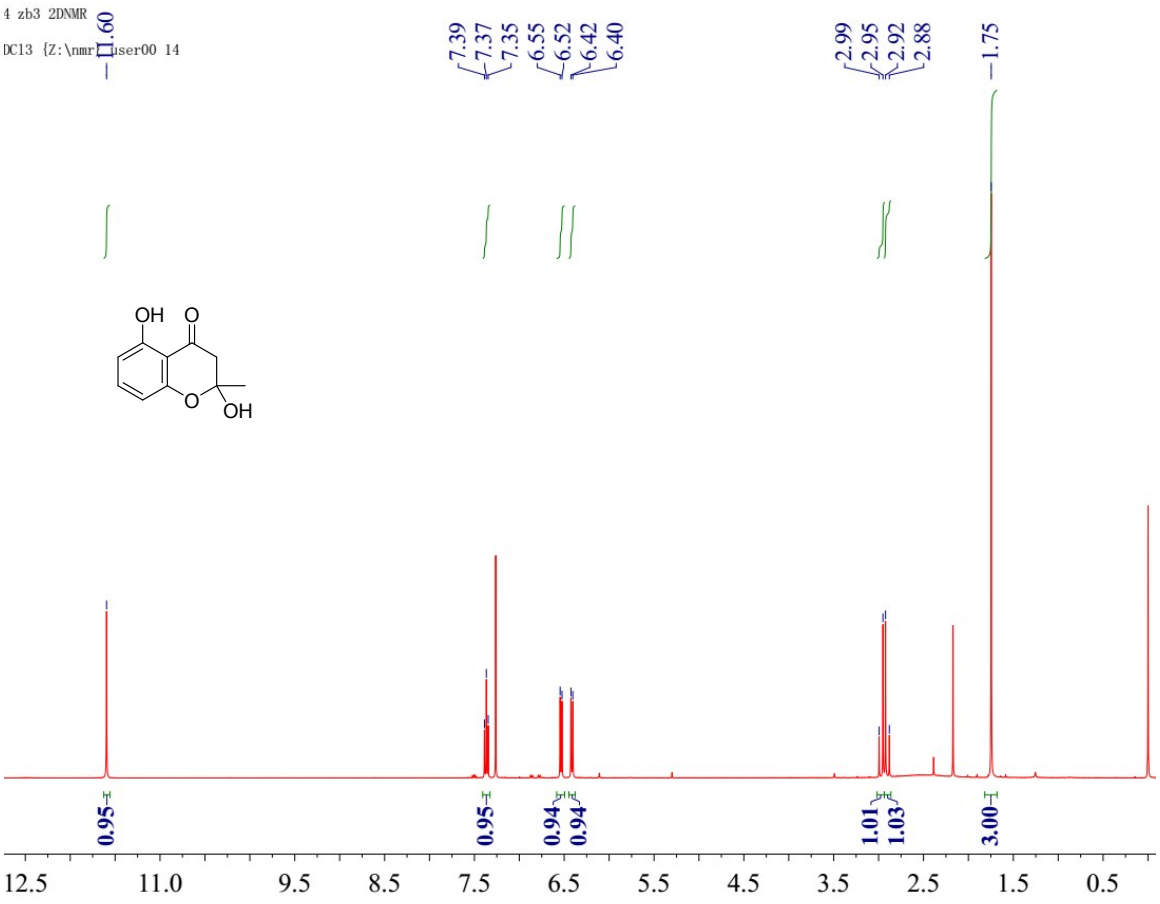

Fig. S31 ^{1}H NMR spectrum of **3** (400 MHz, $CDCl_3$)

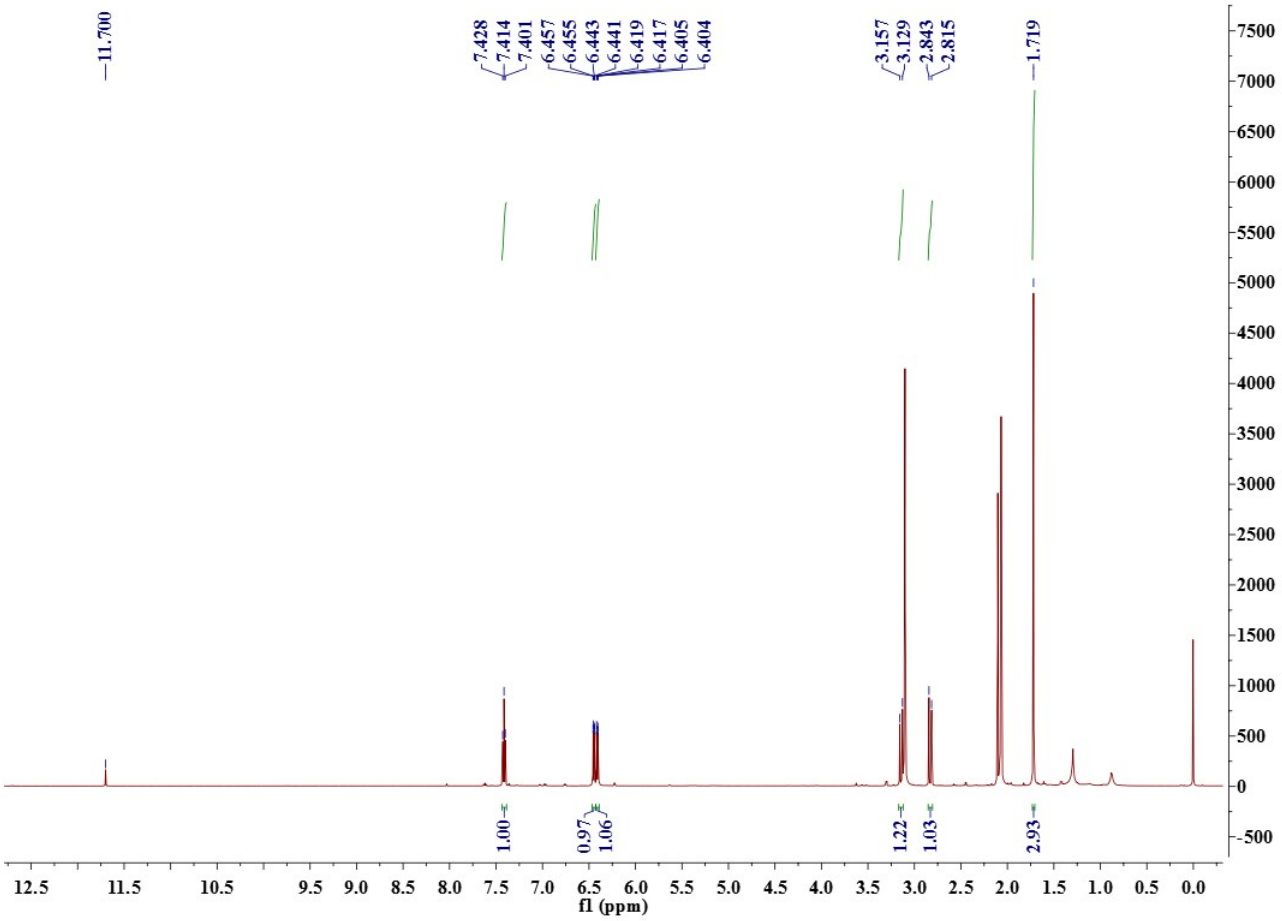

Fig. S32 ^{1}H NMR spectrum of **3** (400 MHz, acetone-d_6)

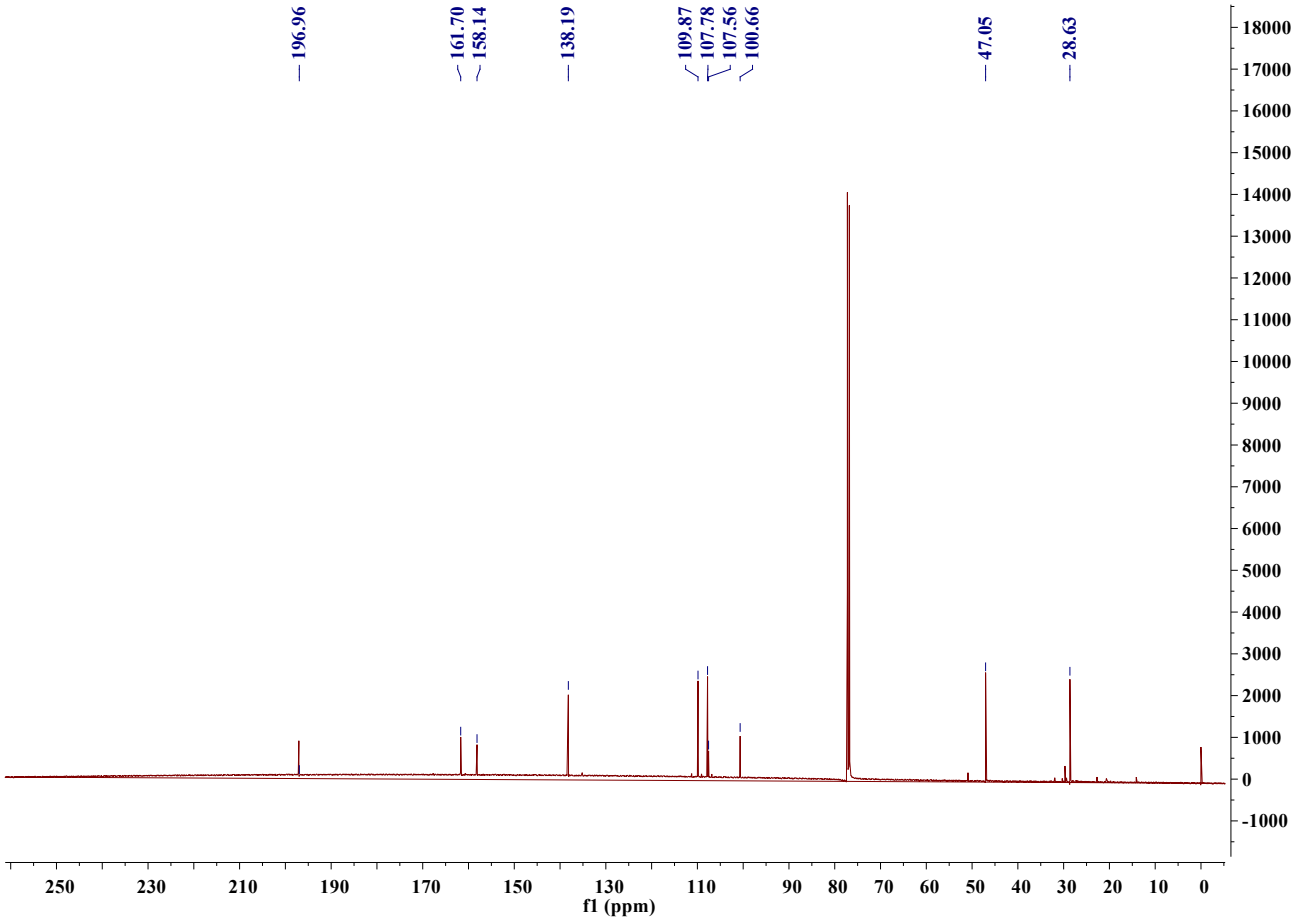

Fig. S33 ^{13}C NMR spectrum of **3** (100 MHz, $CDCl_3$)

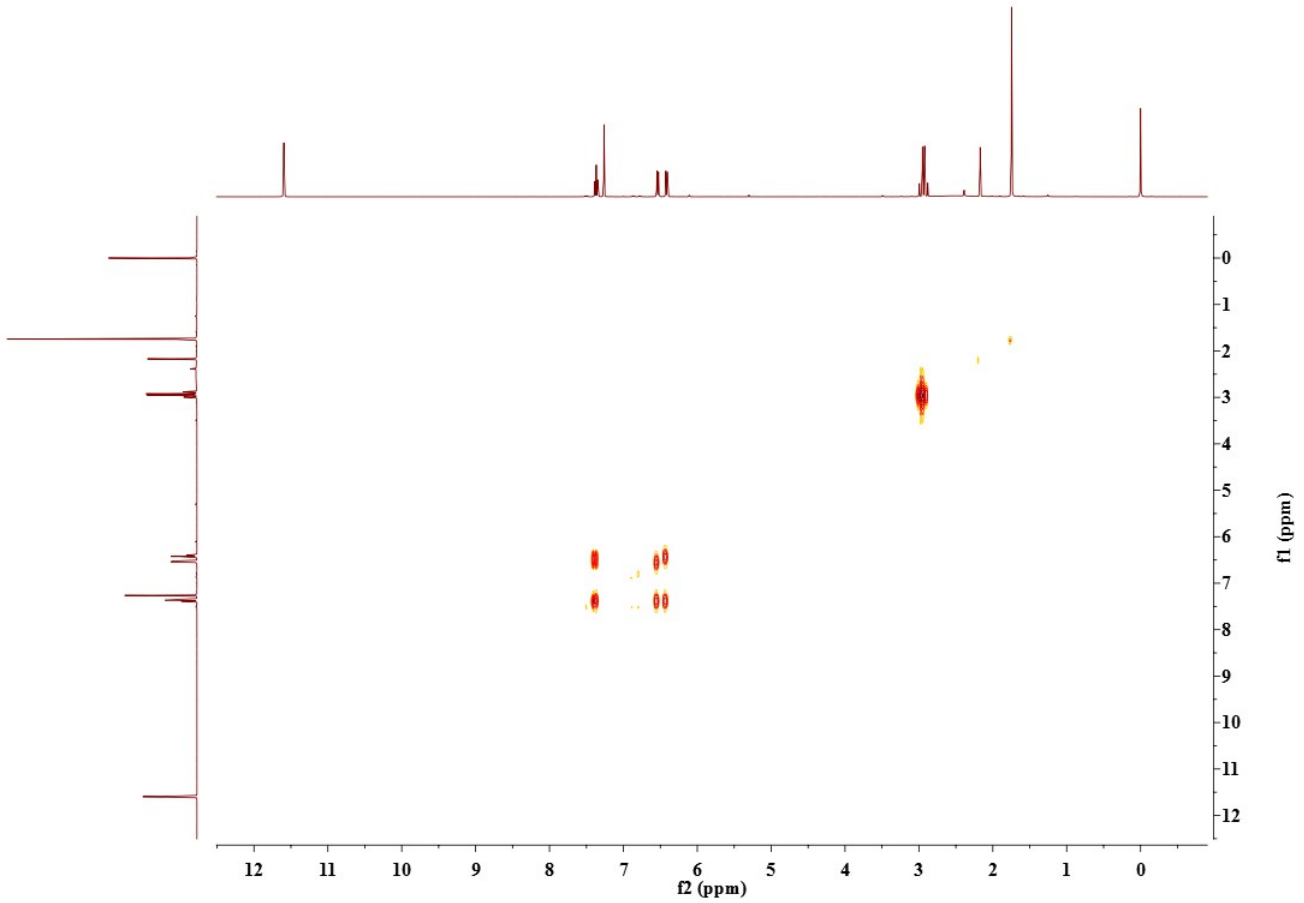

Fig. S34 ^{1}H-^{1}H COSY spectrum of **3** ($CDCl_3$)

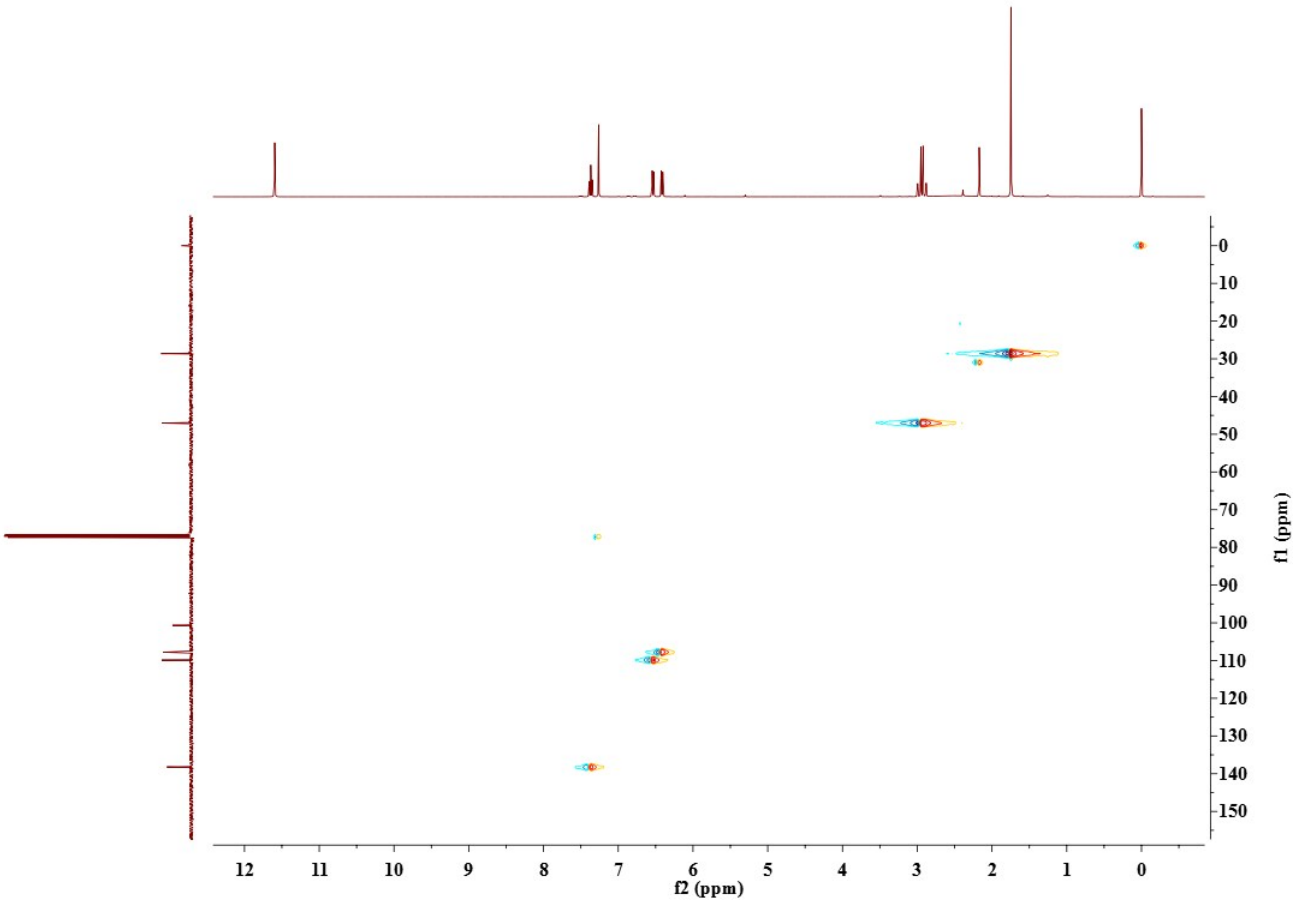

Fig. S35 HSQC spectrum of **3** ($CDCl_3$)

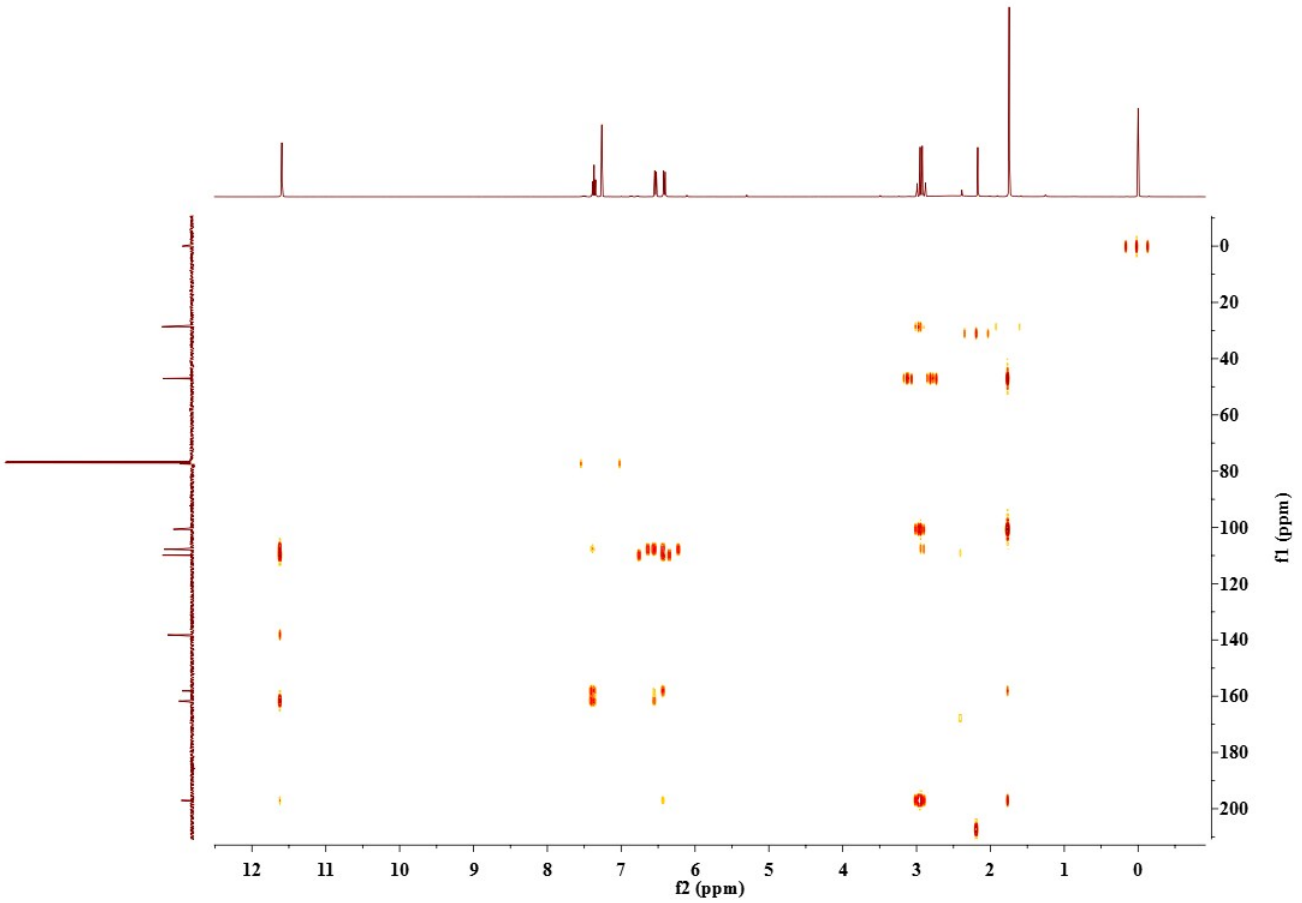

Fig. S36 HMBC spectrum of **3** ($CDCl_3$)

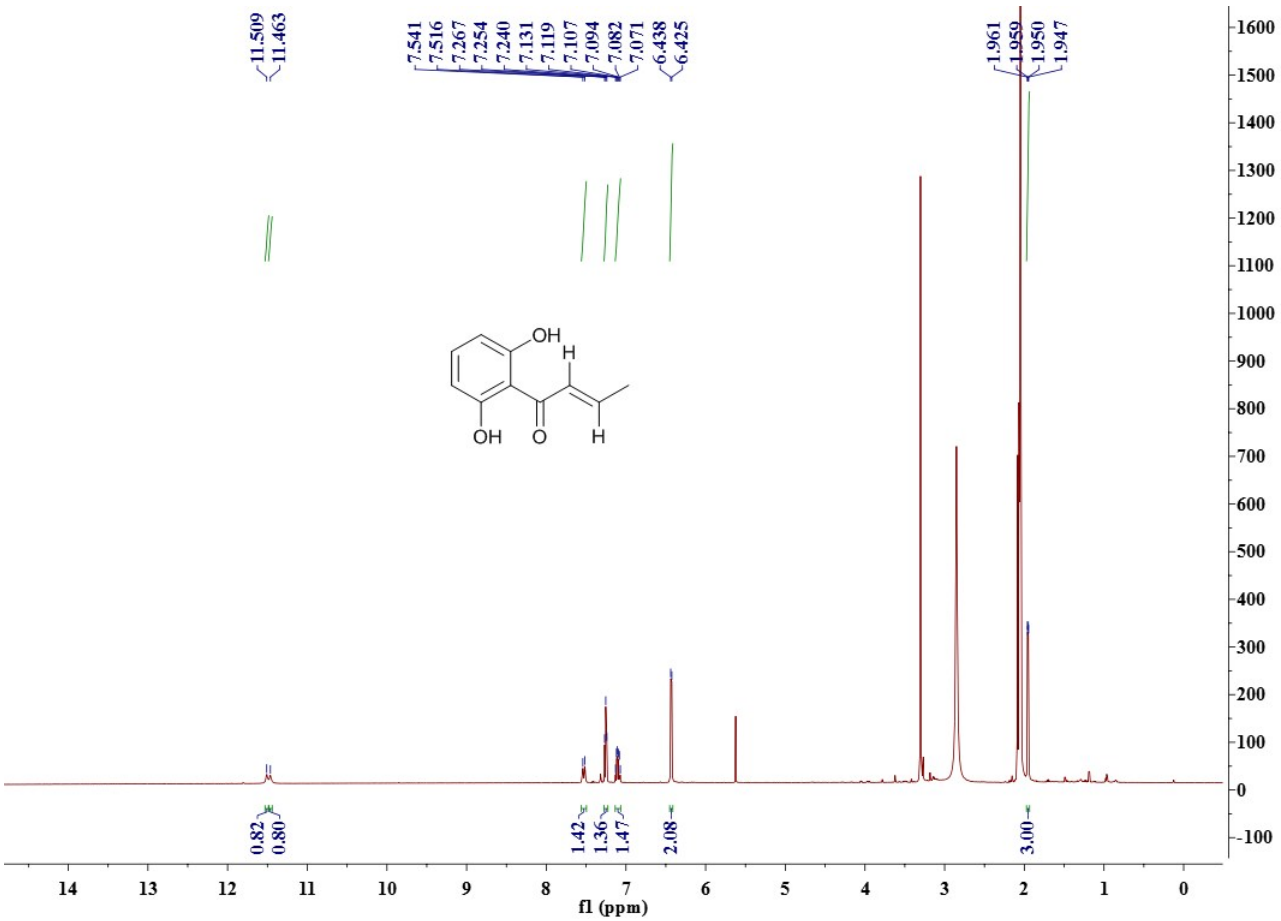

Fig. S37 ^{1}H NMR spectrum of **4** (600 MHz, acetone-d_6)

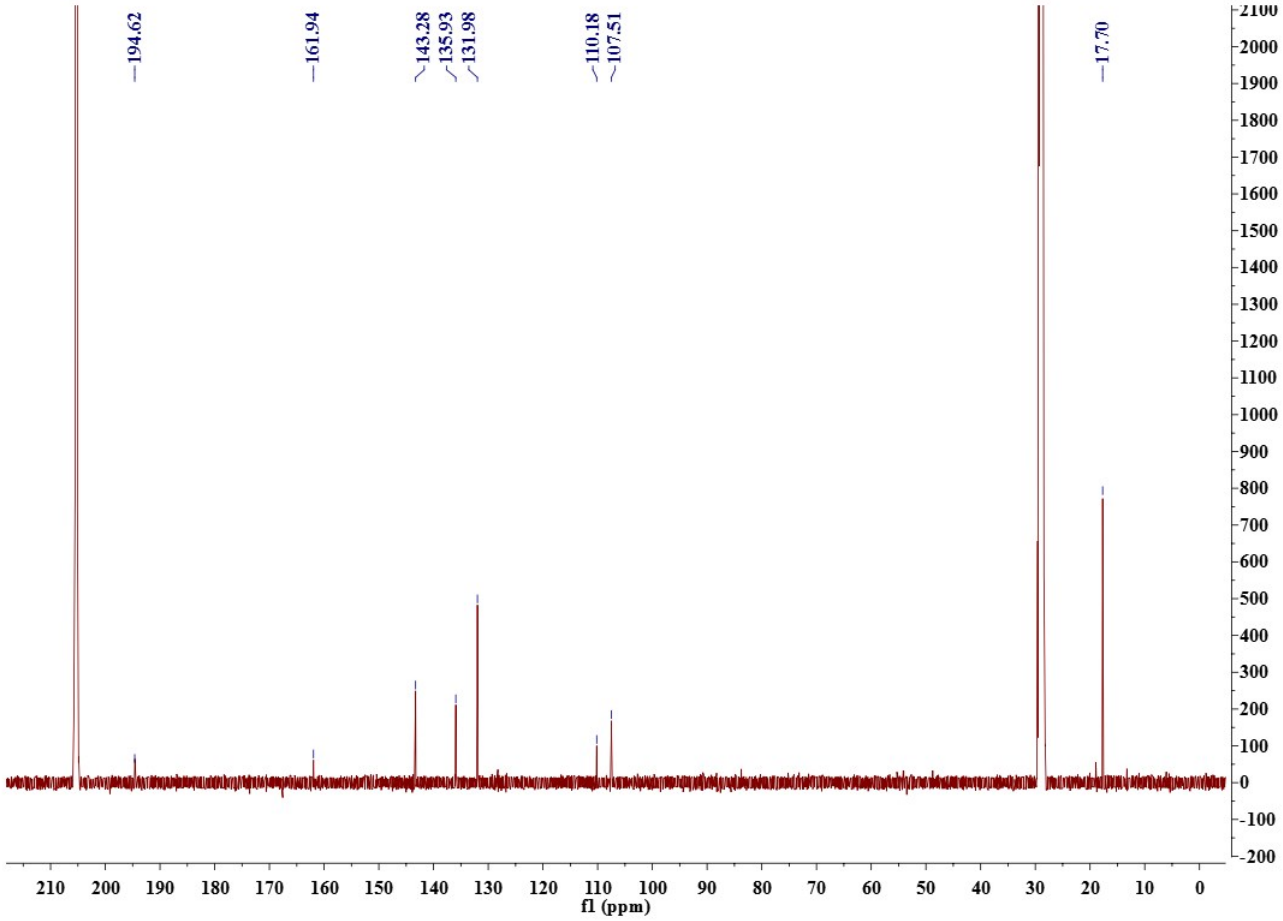

Fig. S38 ^{13}C NMR spectrum of **4** (125 MHz, acetone-d_6)

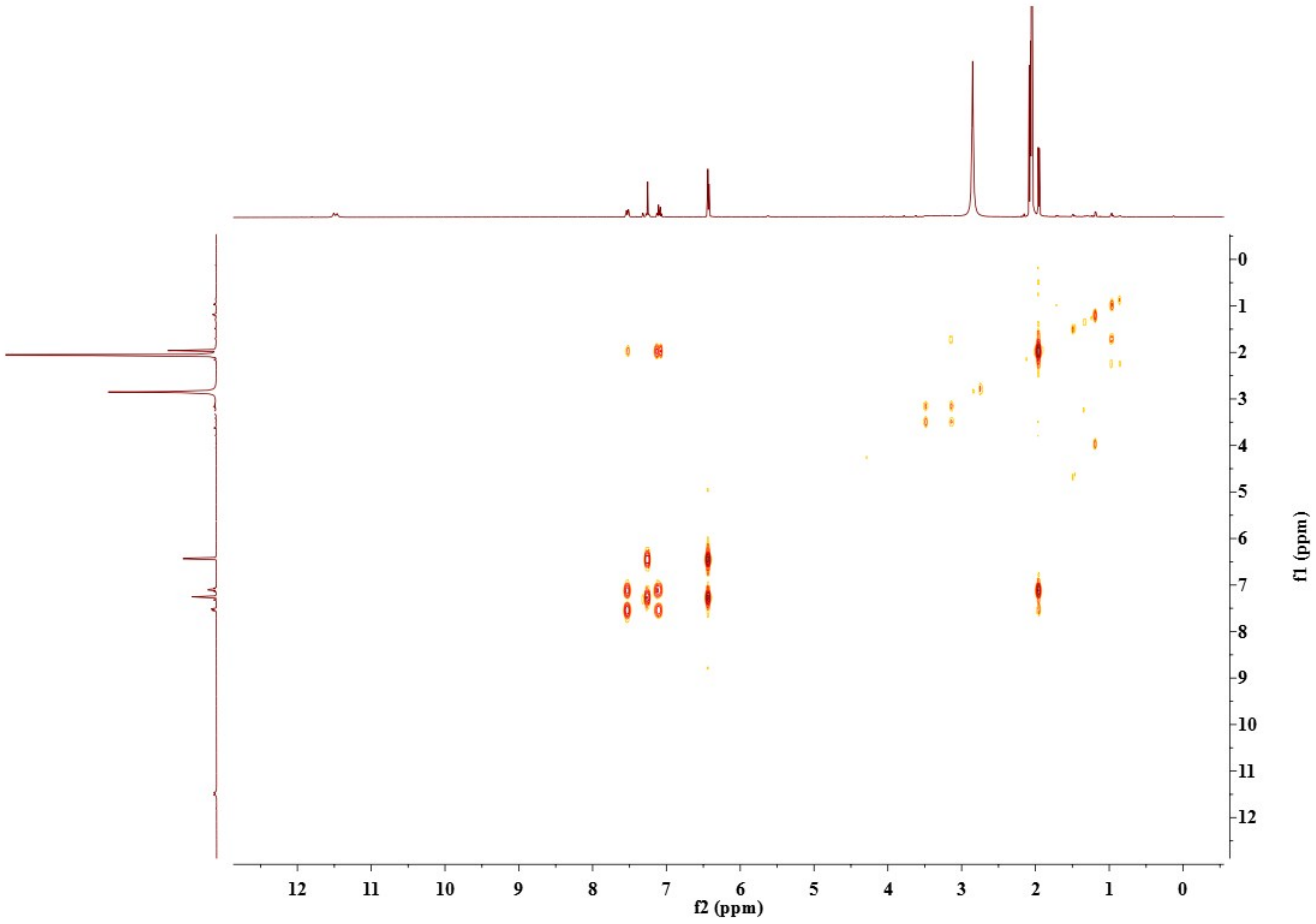

Fig. S39 ^{1}H-^{1}H COSY spectrum of **4** (acetone-d_6)

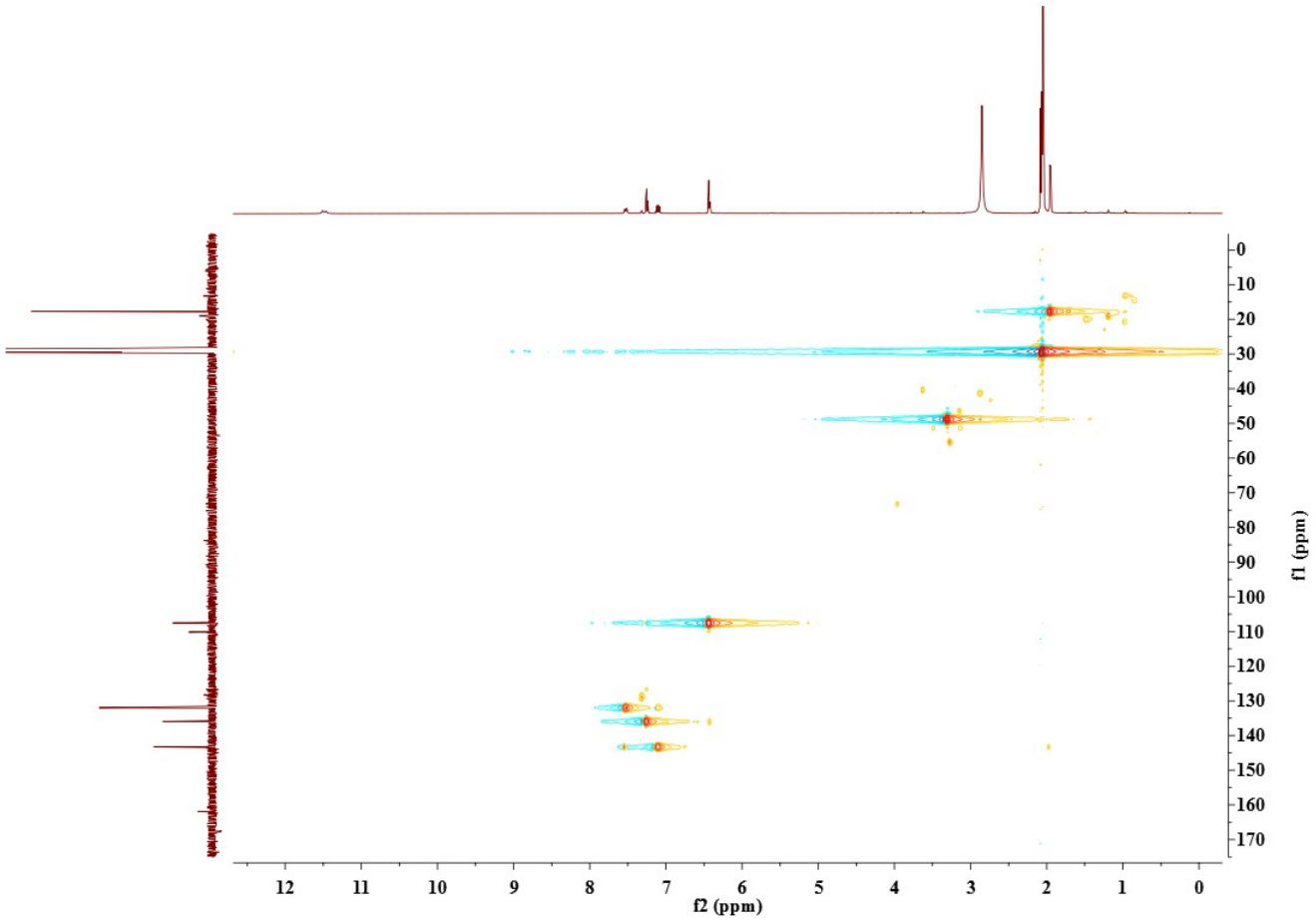

Fig. S40 HSQC spectrum of **4** (acetone-d_6)

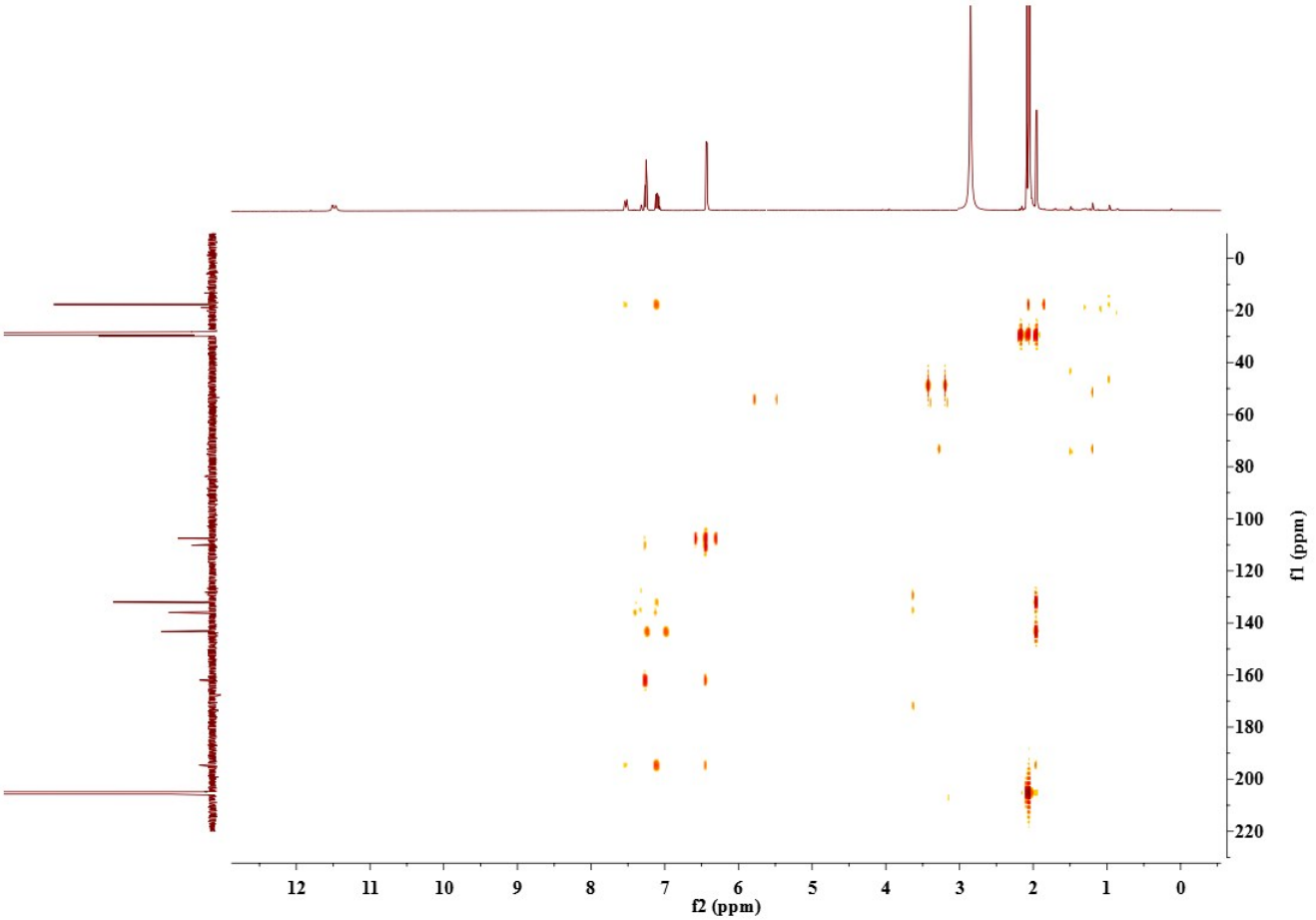

Fig. S41 HMBC spectrum of **4** (acetone-d_6)

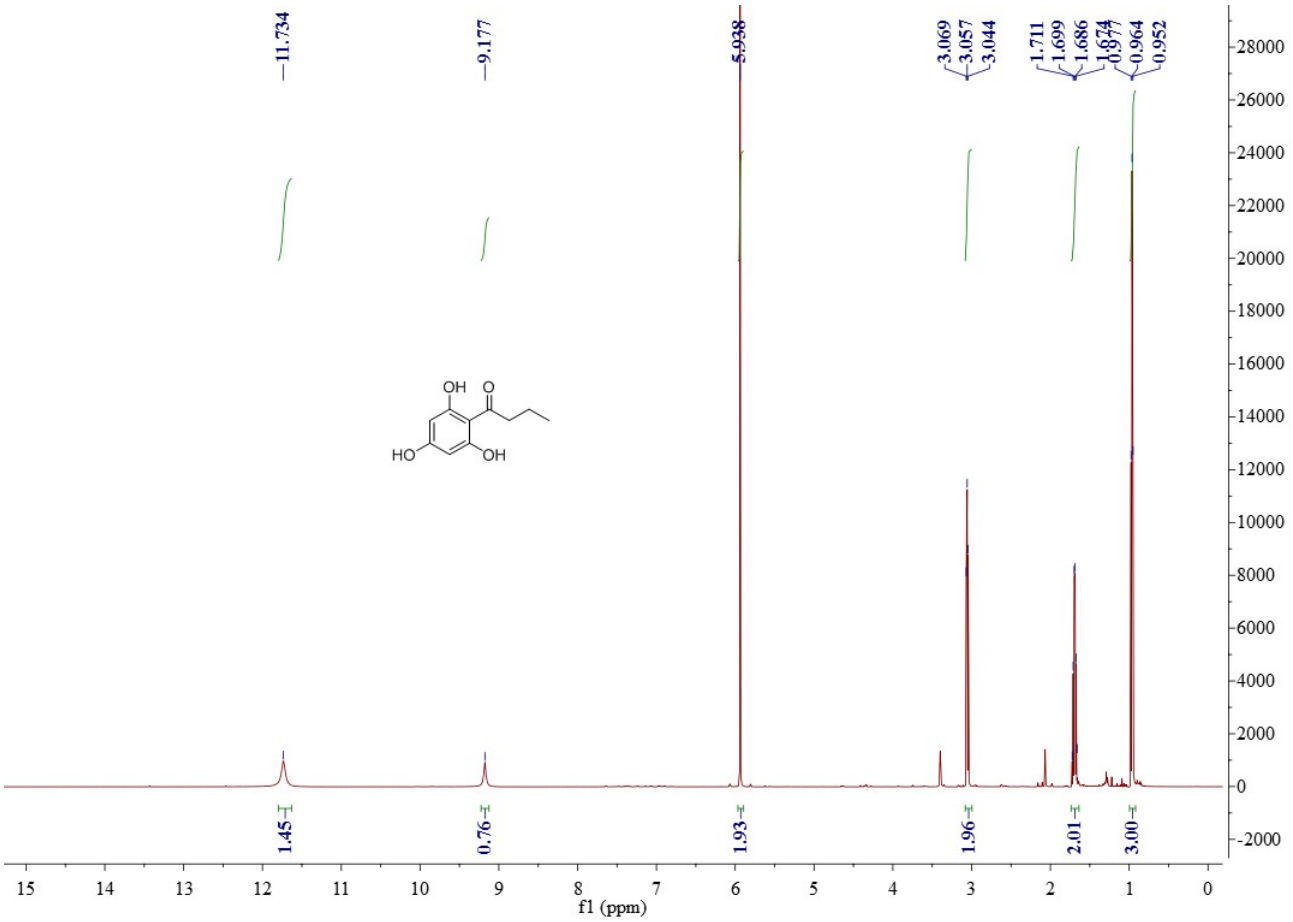

Fig. S42 ^{1}H NMR spectrum of **9** (600 MHz, acetone-d_6)

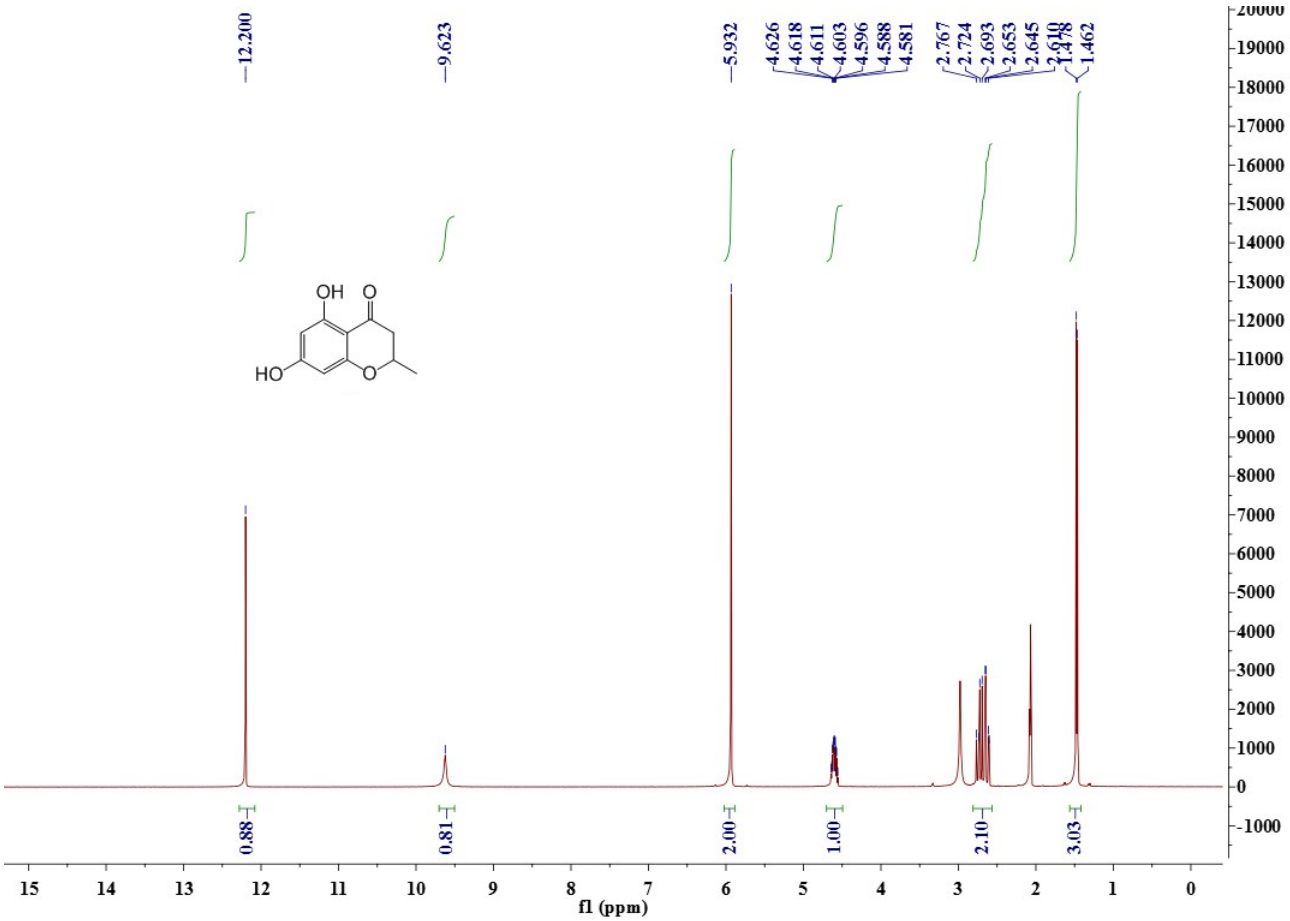

Fig. S43 ^{1}H NMR spectrum of **10** (400 MHz, acetone-d_6)

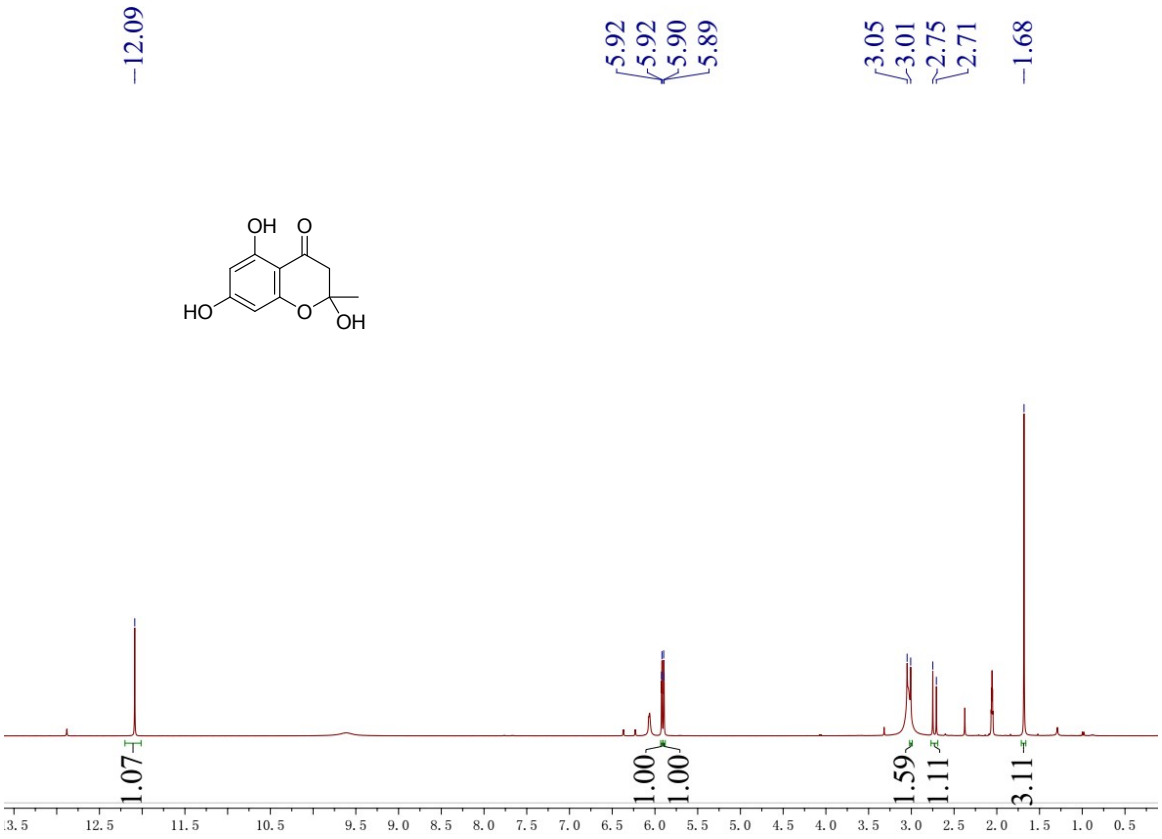

Fig. S44 ^{1}H NMR spectrum of **13** (400 MHz, acetone-d_6)

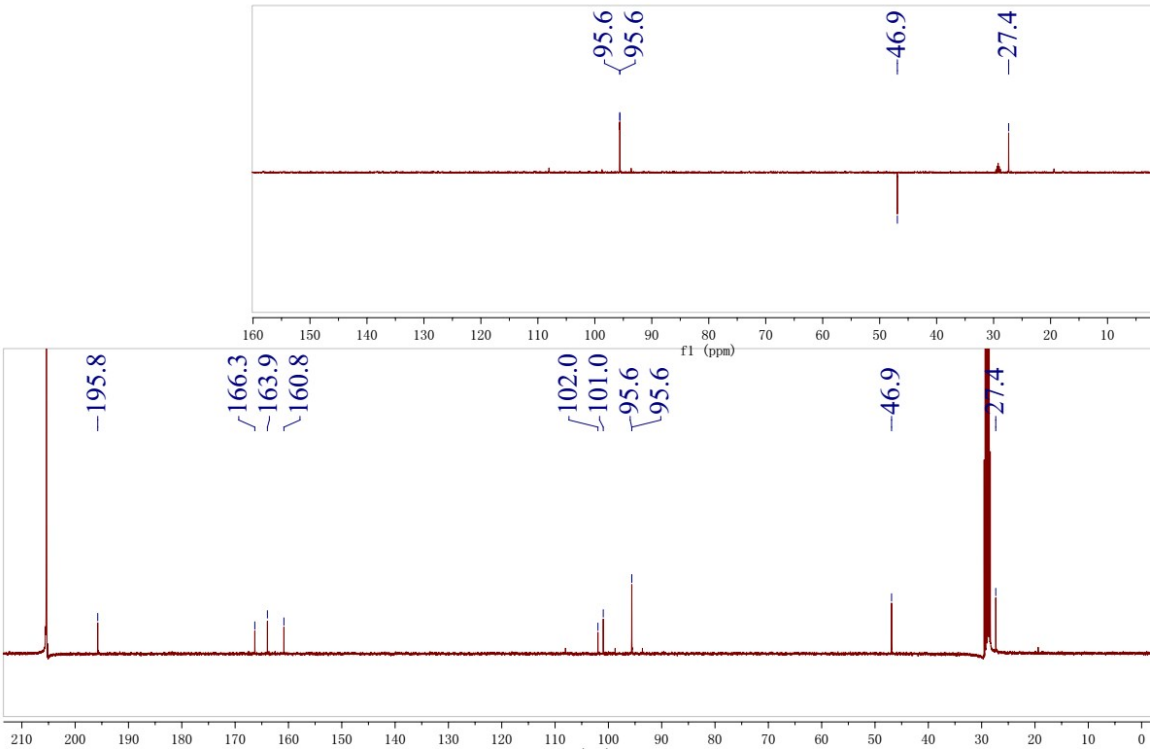

Fig. S45 ^{13}C NMR and DEPT spectra of **13** (100 MHz, acetone-d_6)

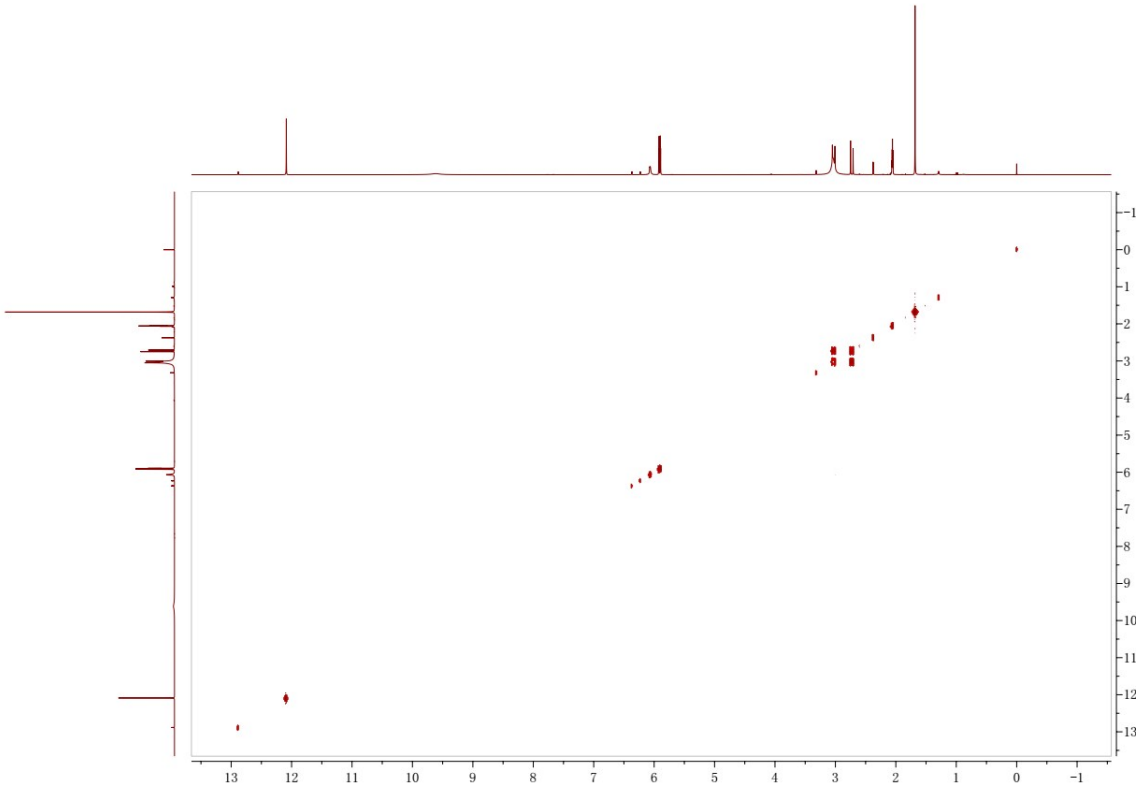

Fig. S46 ^{1}H-^{1}H COSY spectrum of **13** (acetone-d_6)

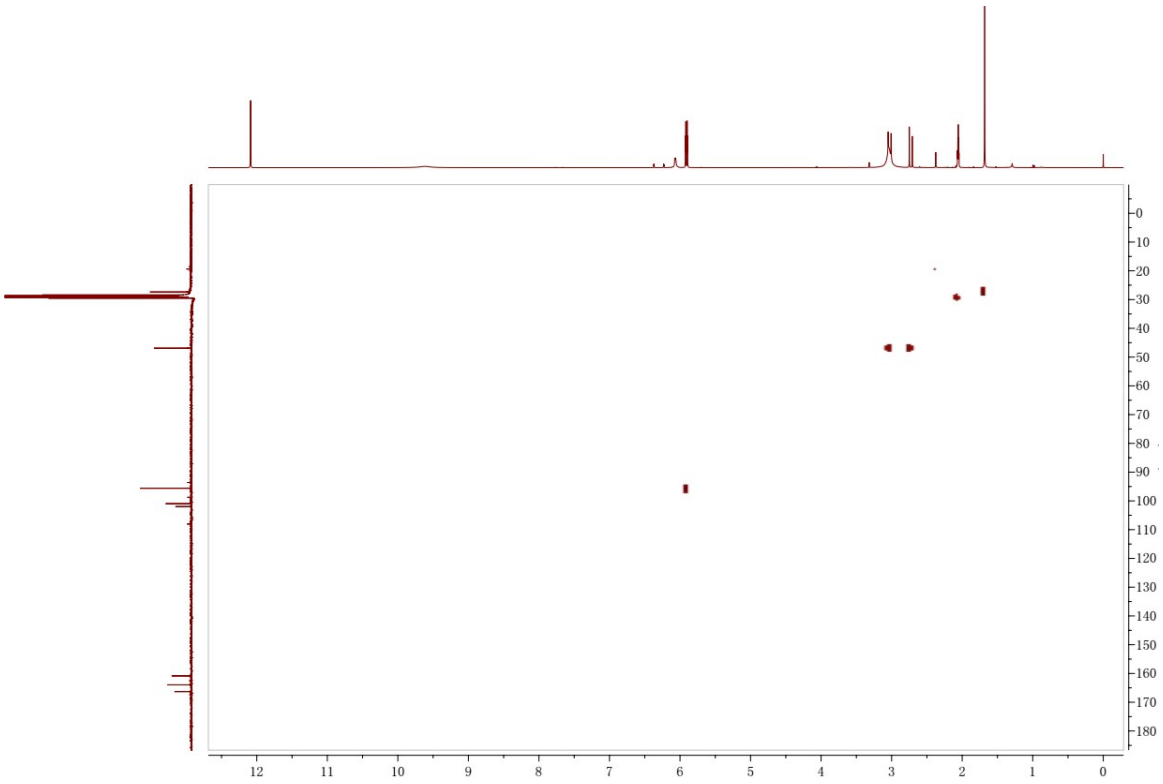

Fig. S47 HSQC spectrum of **13** (acetone-d_6)

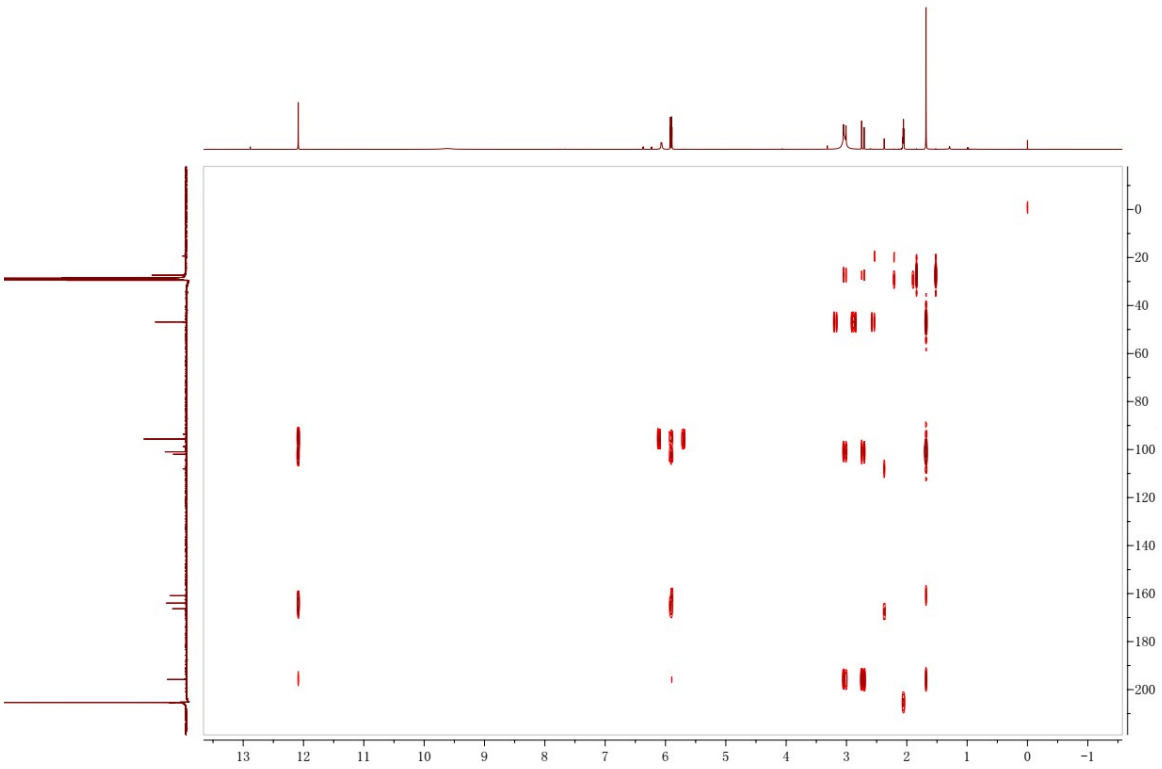

Fig. S48 HMBC spectrum of **13** (acetone-d_6)

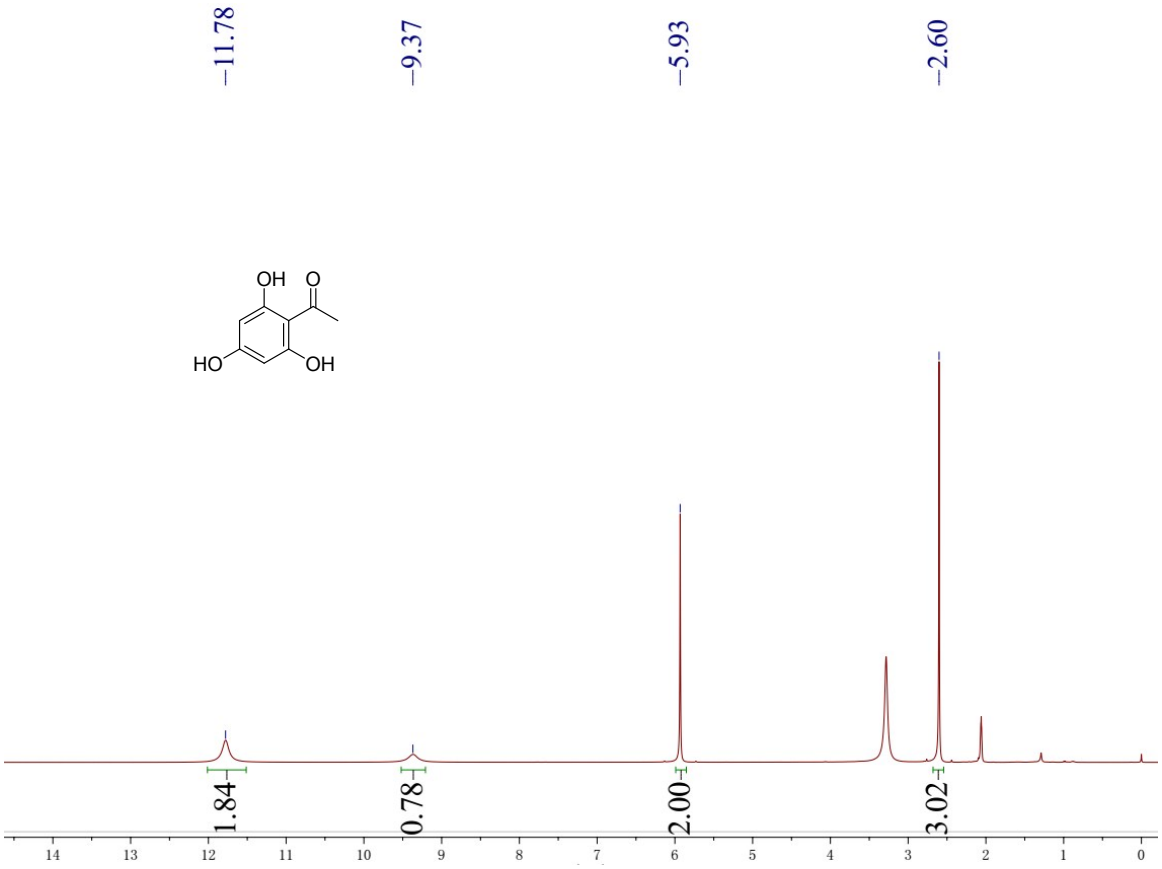

Fig. S49 ^{1}H NMR spectrum of **14** (400 MHz, acetone-d_6)

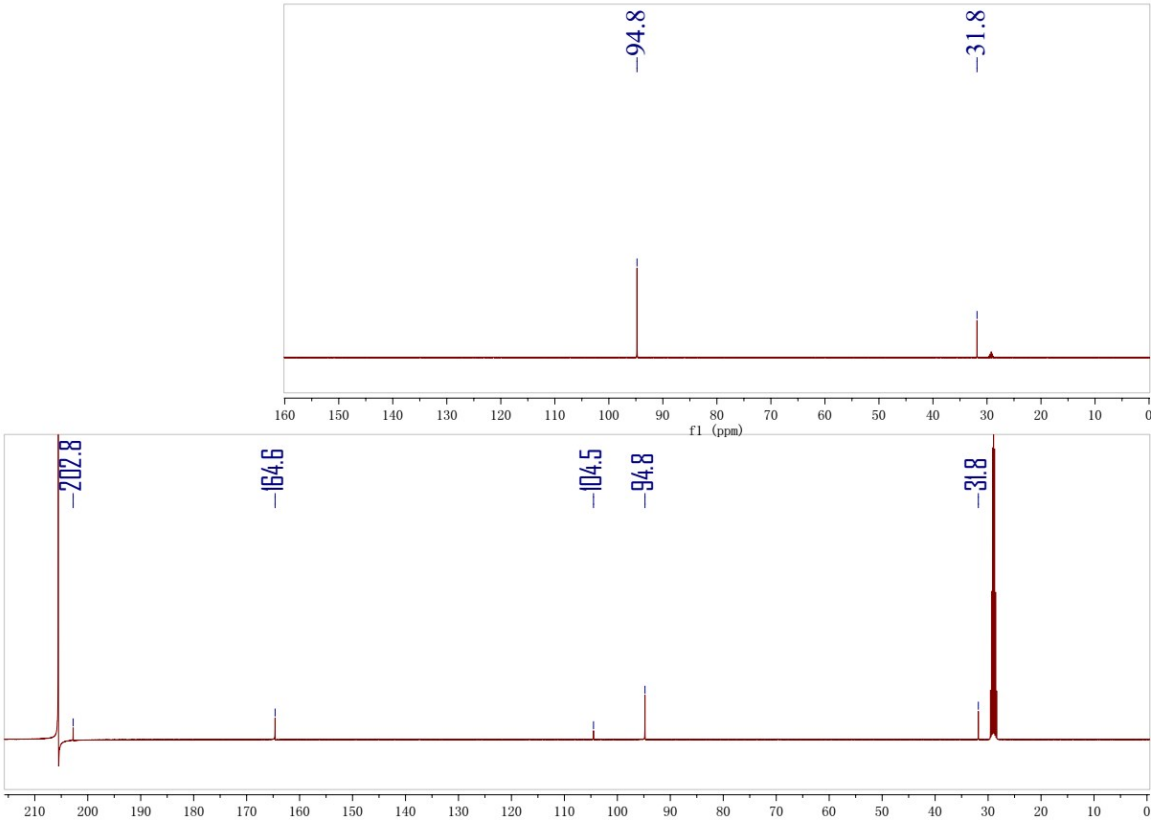

Fig. S50 ^{13}C NMR and DEPT spectra of **14** (100 MHz, acetone-d_6)

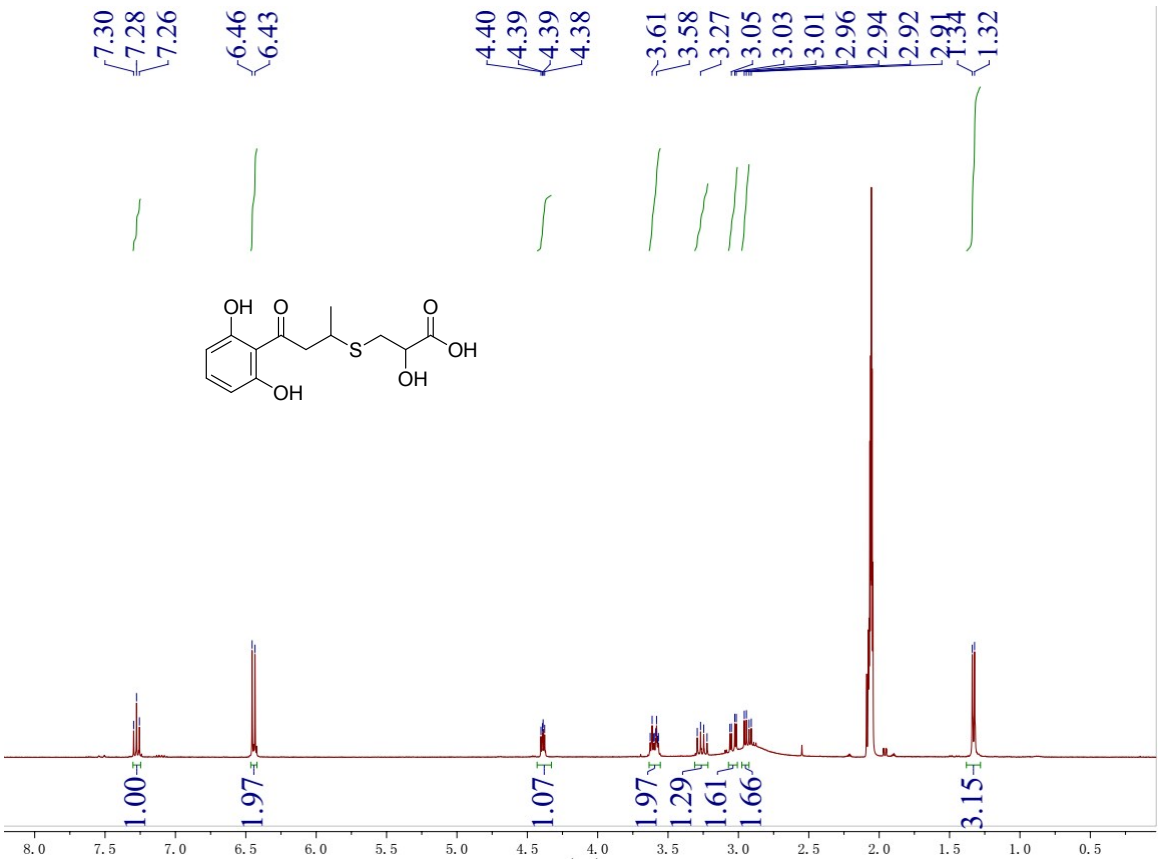

Fig. S51 ^{1}H NMR spectrum of **15** (400 MHz, acetone-d_6)

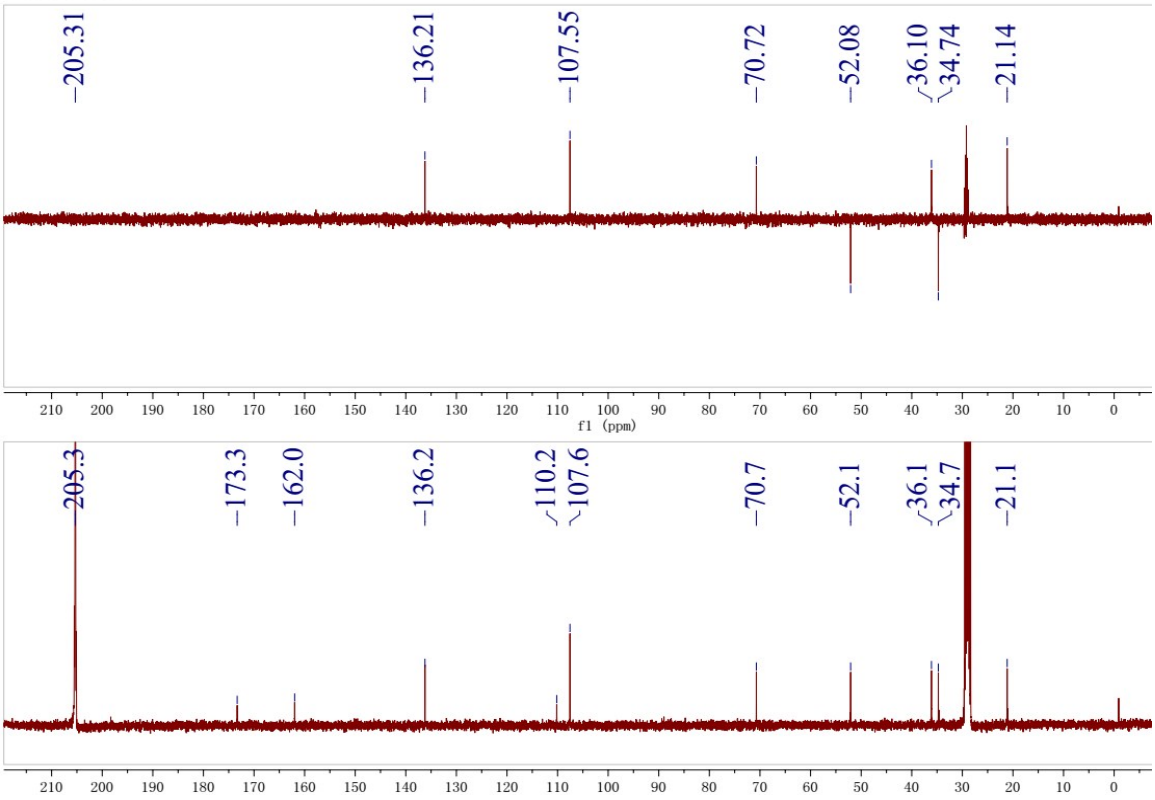

Fig. S52 ^{13}C NMR and DEPT spectra of **15** (100 MHz, acetone-d_6)

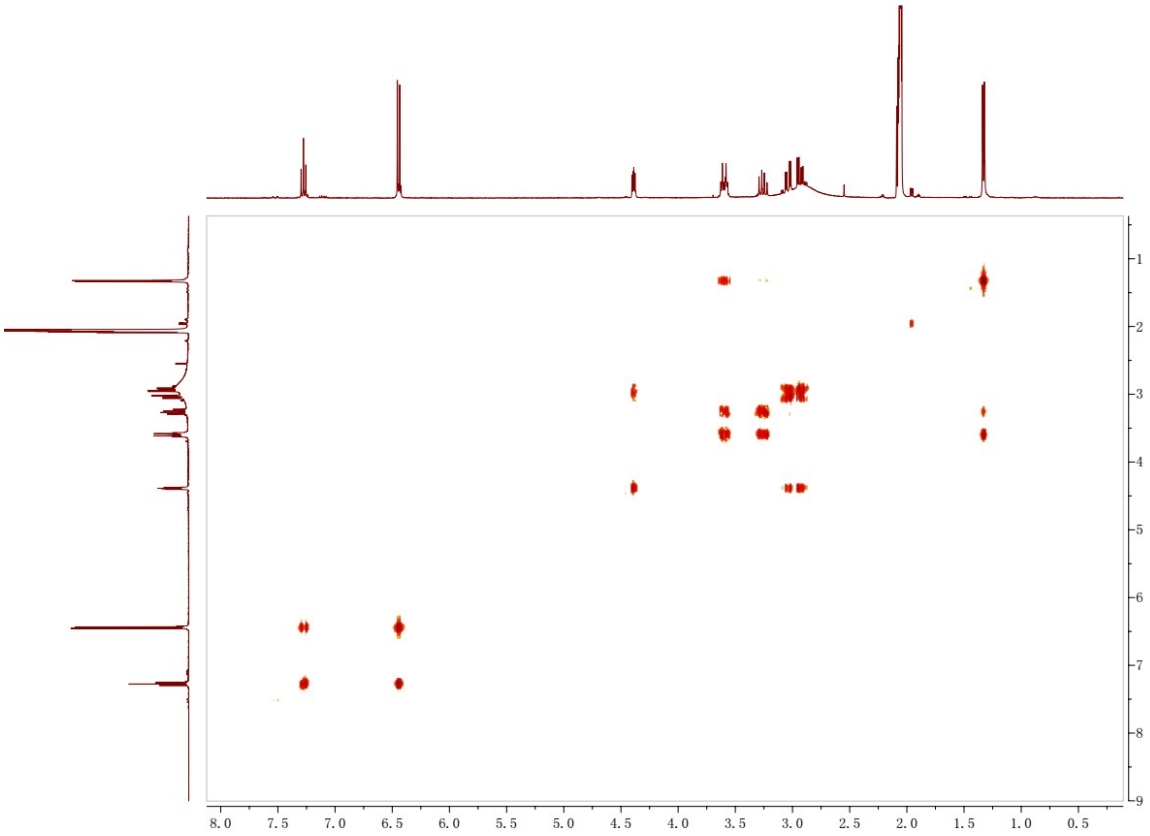

Fig. S53 ^{1}H-^{1}H COSY spectrum of **15** (acetone-d_6)

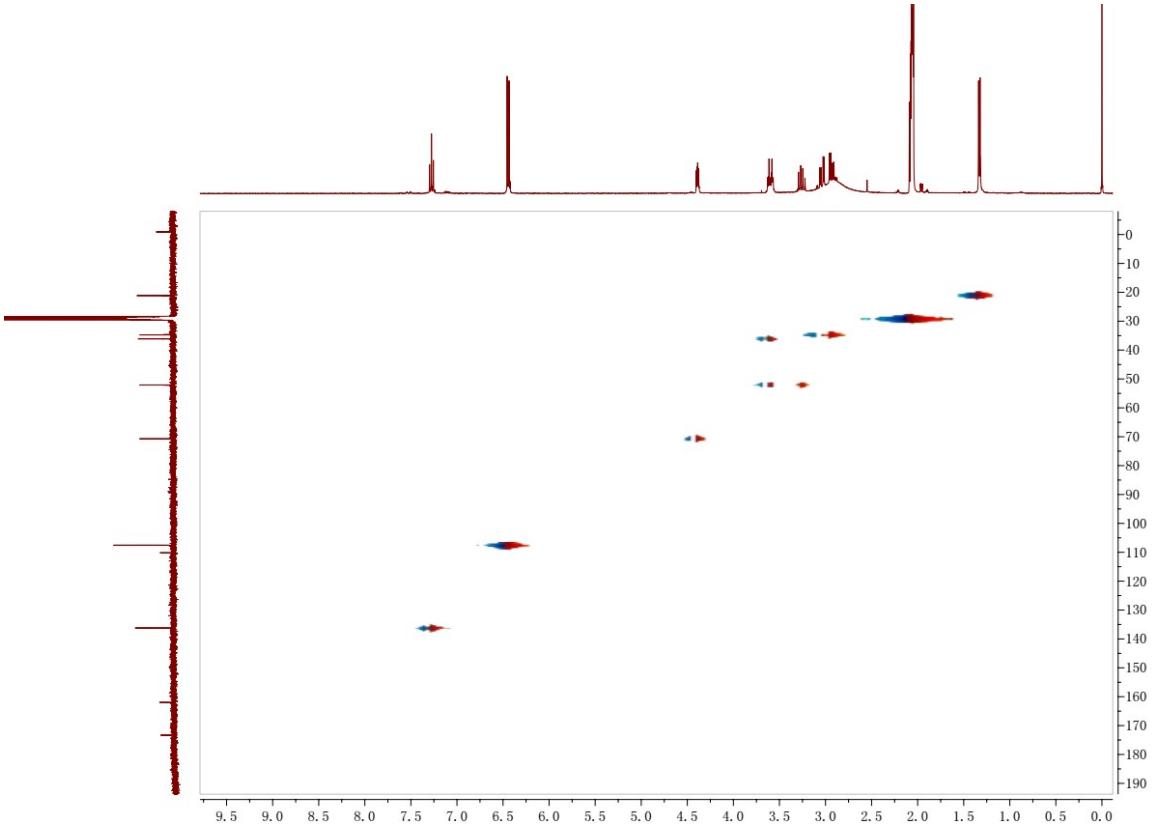

Fig. S54 HSQC spectrum of **15** (acetone-d_6)

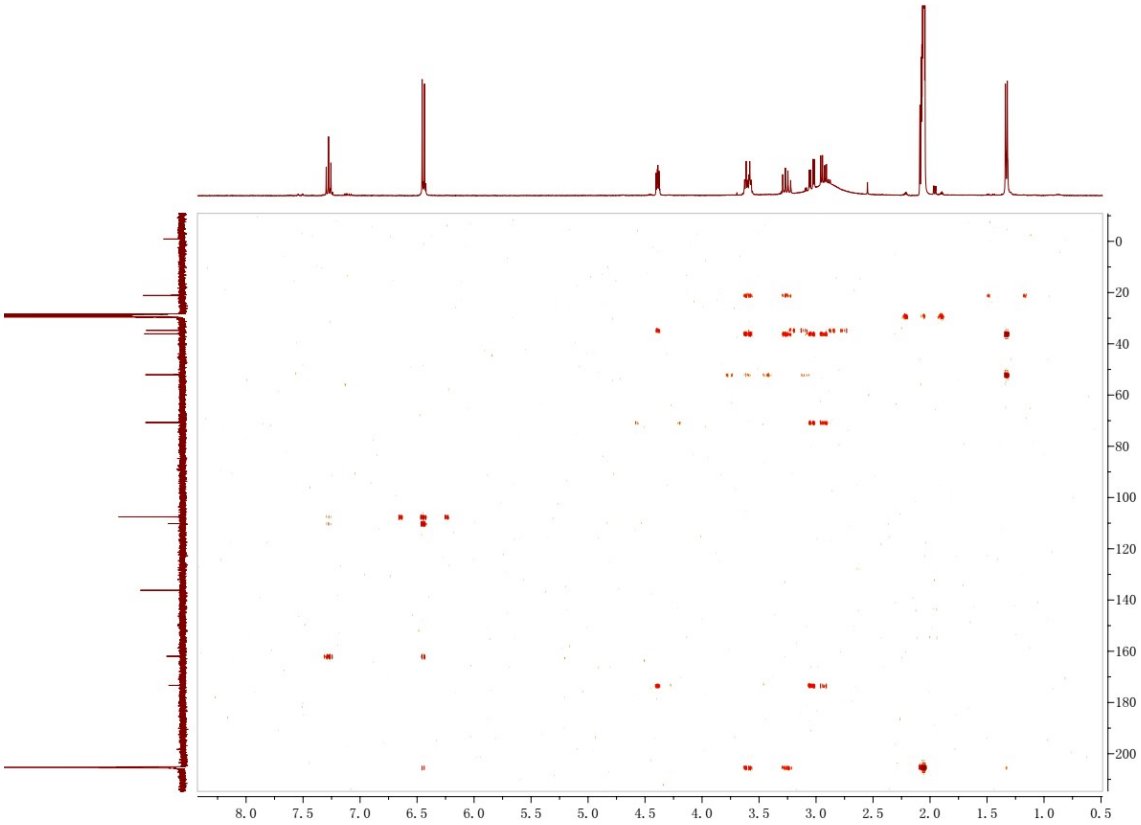

Fig. S55 HMBC spectrum of **15** (acetone-d_6)

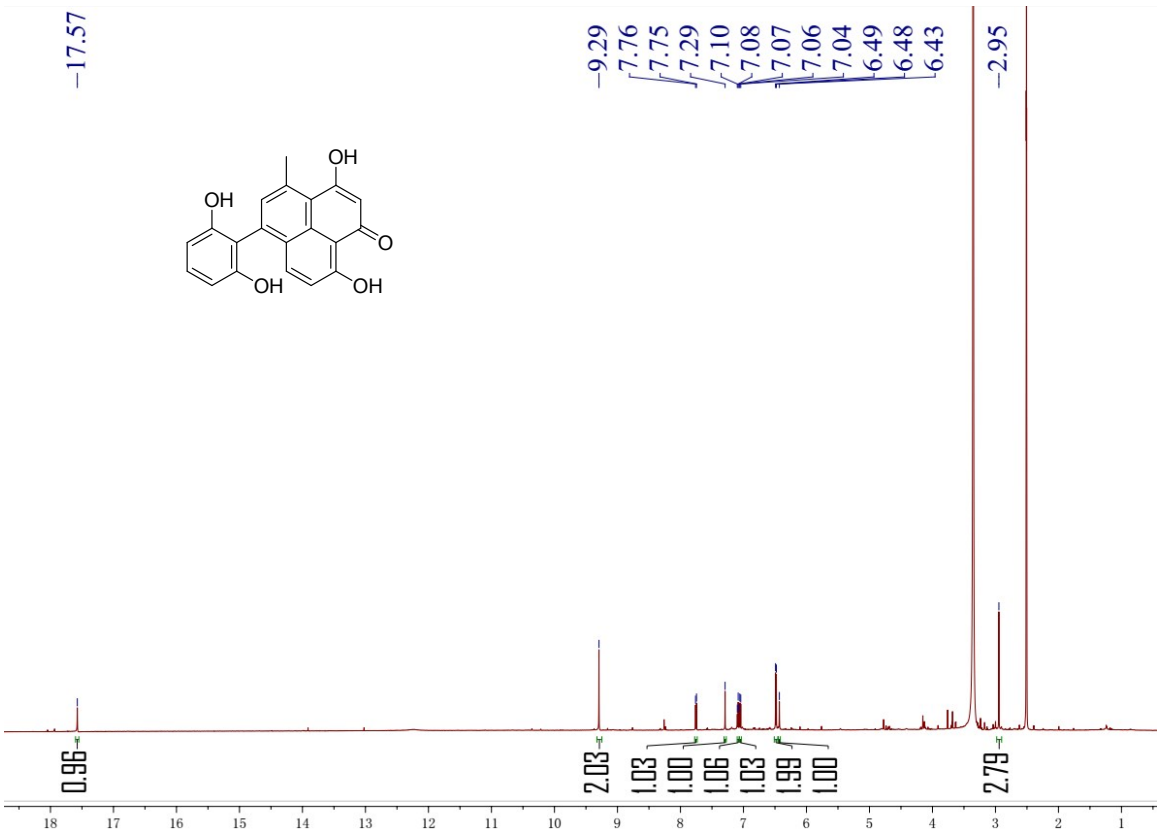

Fig. S56 ^{1}H NMR spectrum of **20a** (600 MHz, DMSO-d_6)

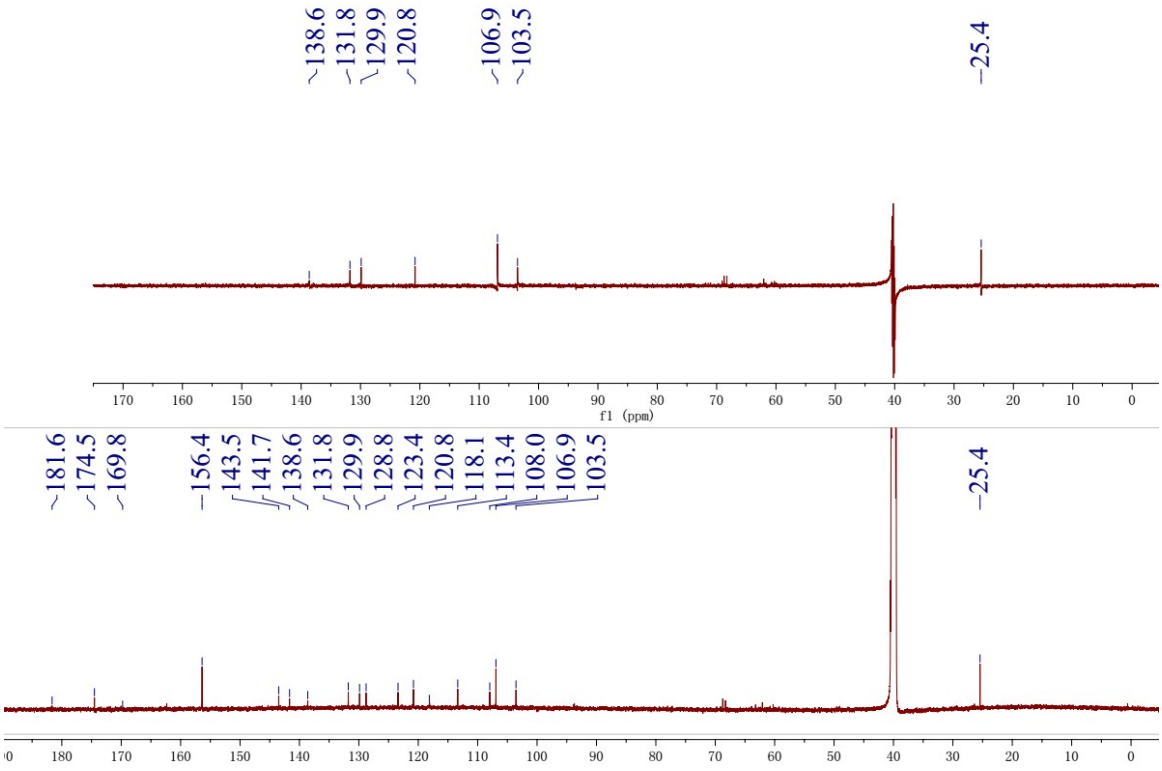

Fig. S57 ^{13}C NMR and DEPT spectra of **20a** (150 MHz, DMSO-d_6)

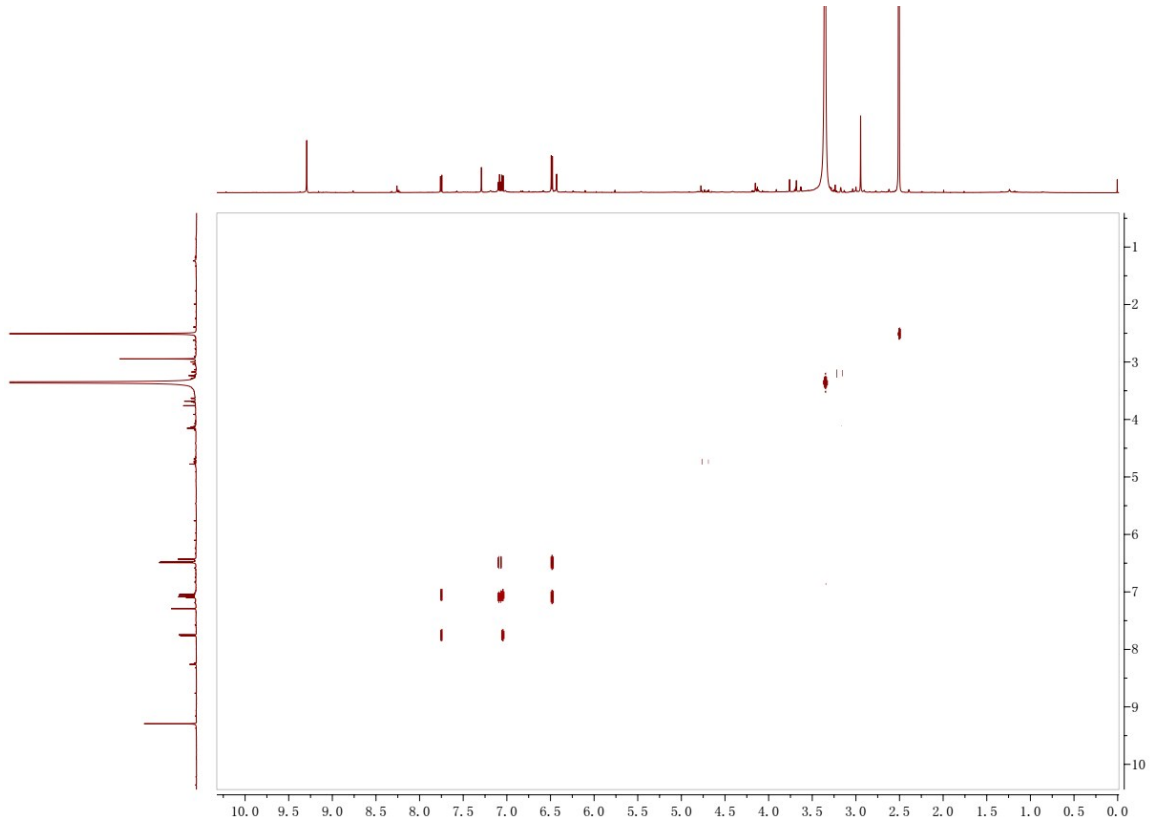

Fig. S58 ^{1}H-^{1}H COSY spectrum of **20a** (DMSO-d_6)

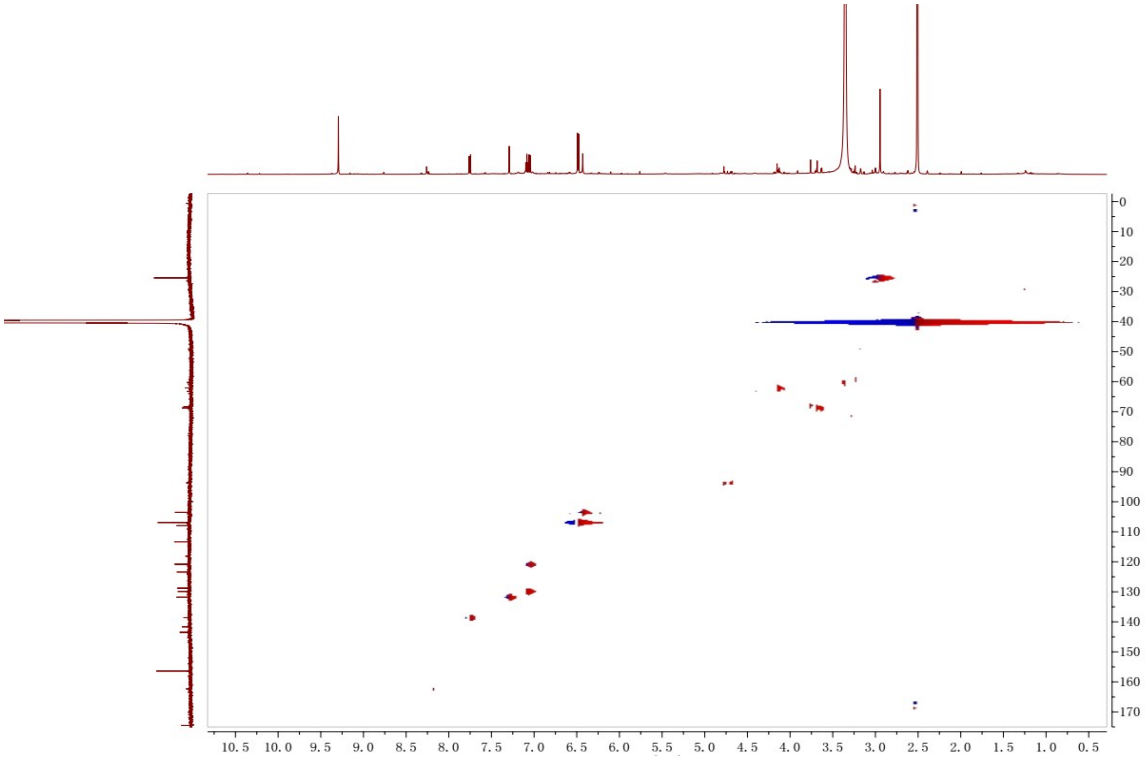

Fig. S59 HSQC spectrum of **20a** (DMSO-d_6)

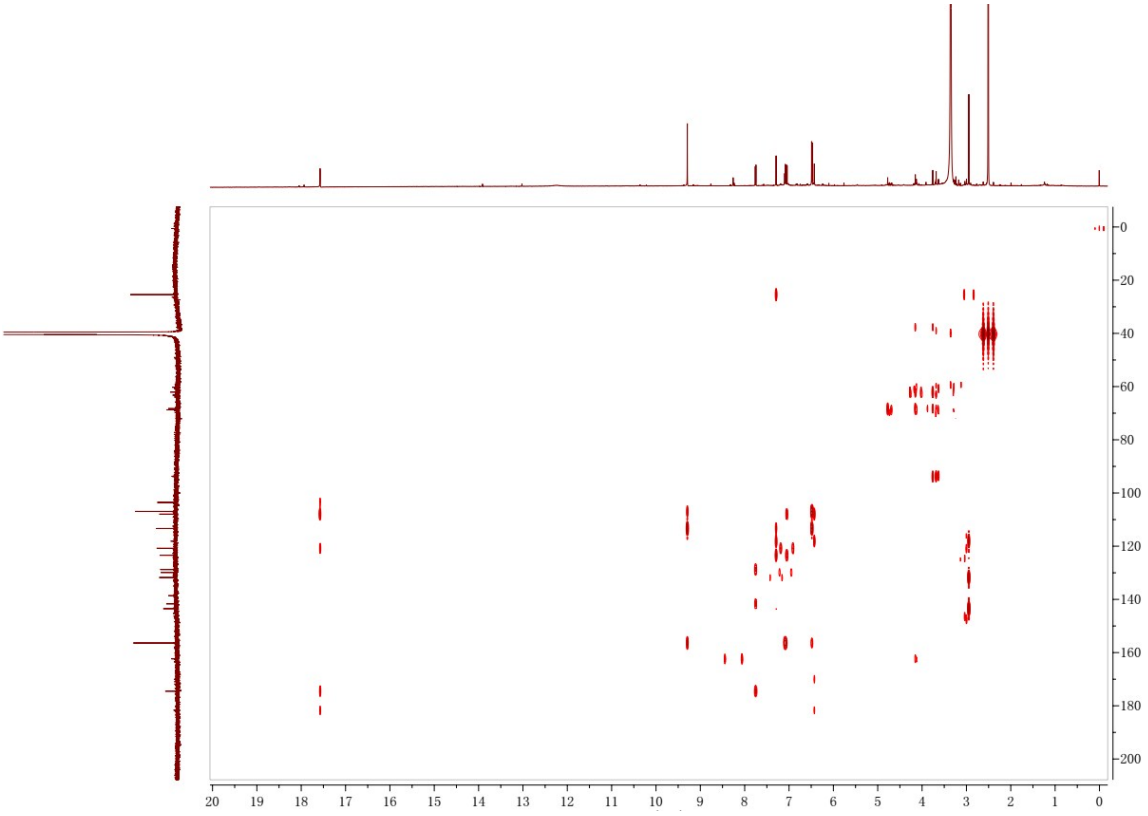

Fig. S60 HMBC spectrum of **20a** (DMSO-d_6)

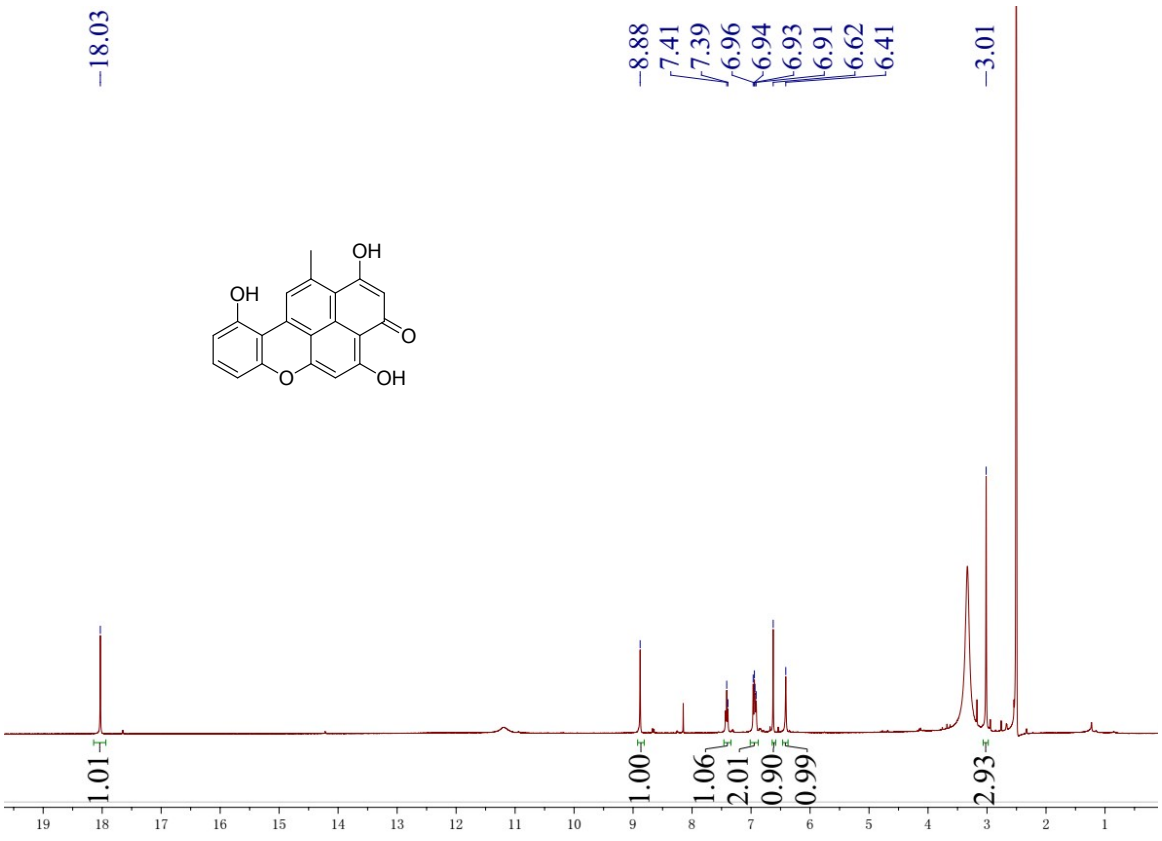

Fig. S61 ^{1}H NMR spectrum of **20b** (400 MHz, DMSO-d_6)

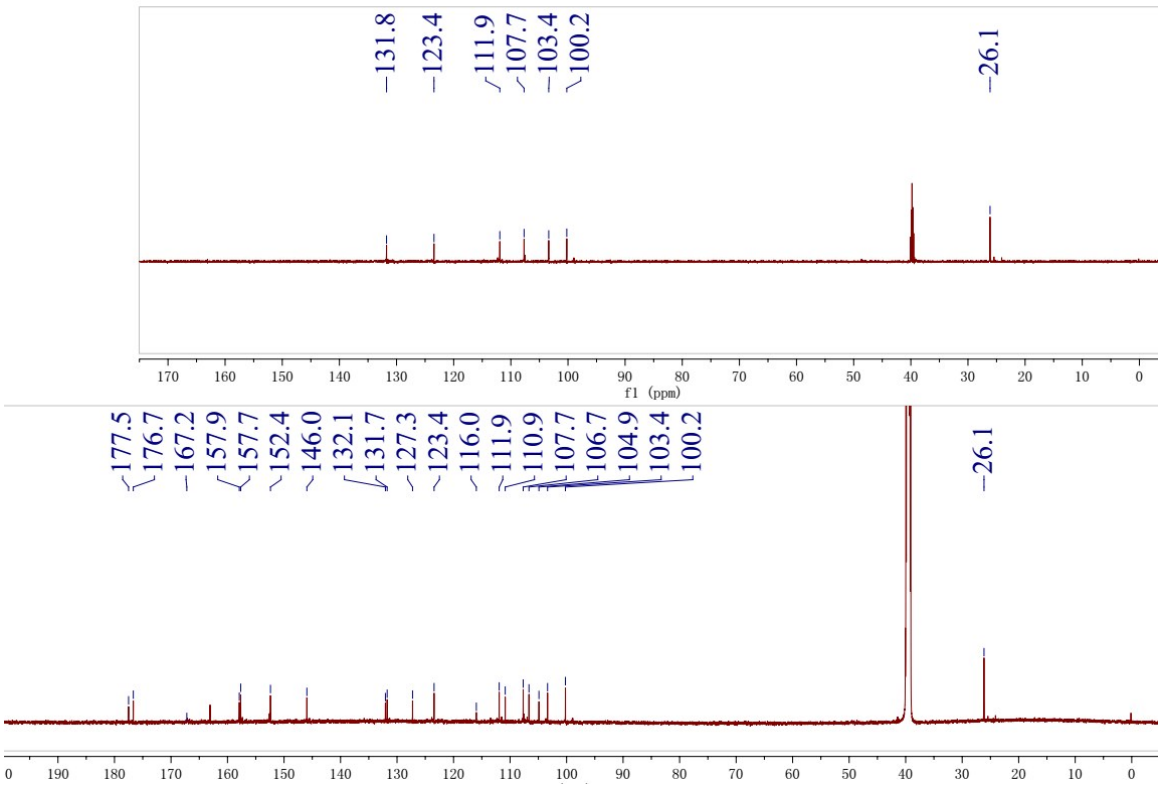

Fig. S62 ^{13}C NMR and DEPT spectra of **20b** (150 MHz, DMSO-d_6)

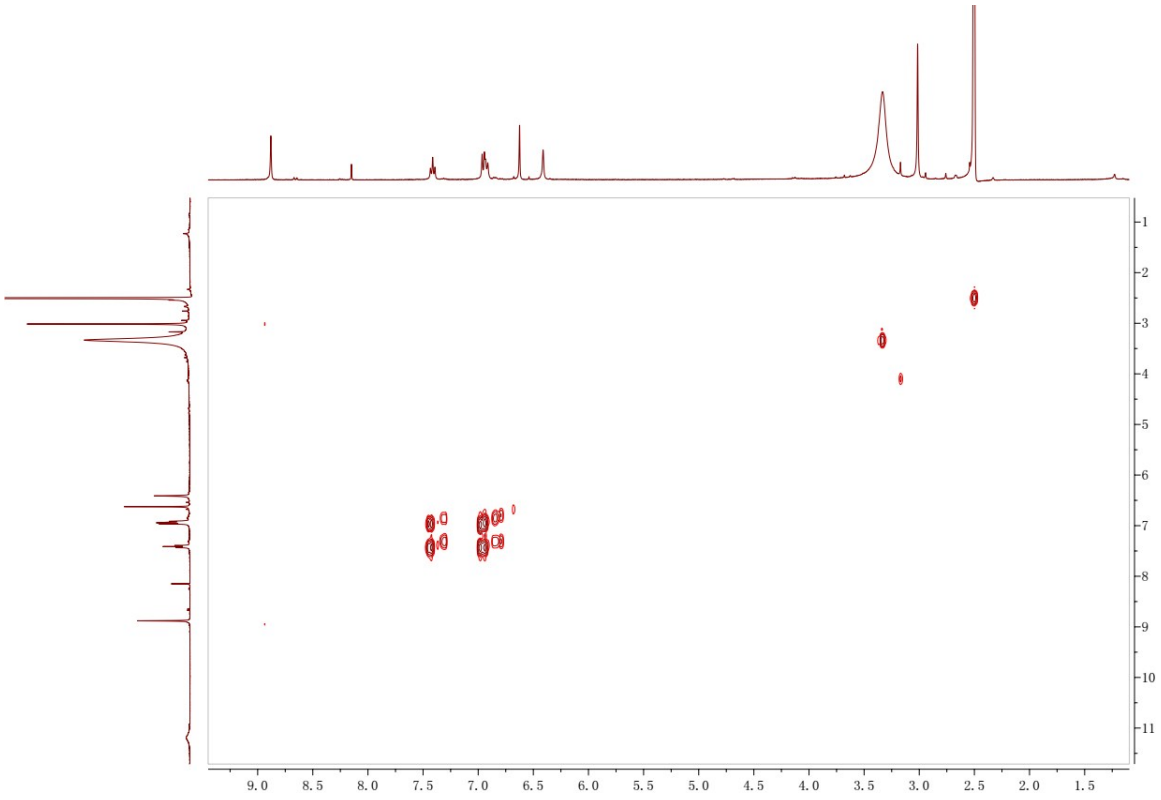

Fig. S63 ^{1}H-^{1}H COSY spectrum of **20b** (DMSO-d_6)

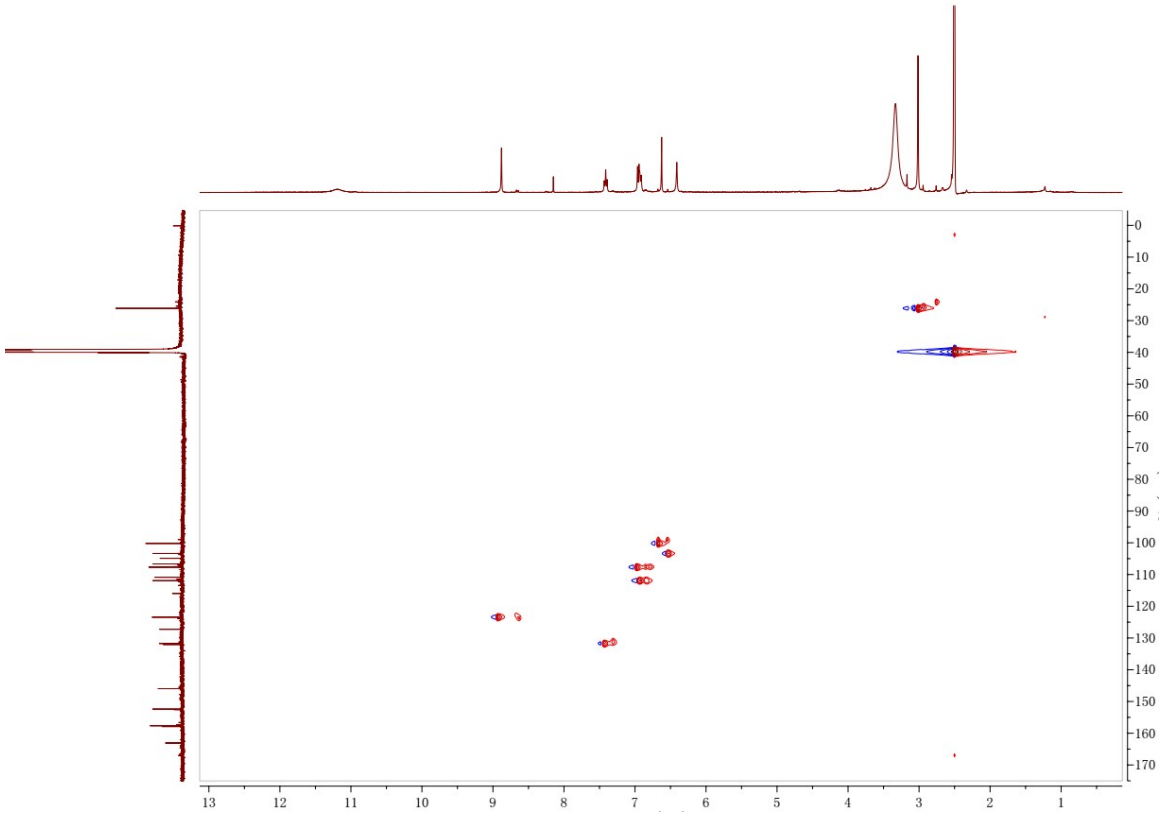

Fig. S64 HSQC spectrum of **20b** (DMSO-d_6)

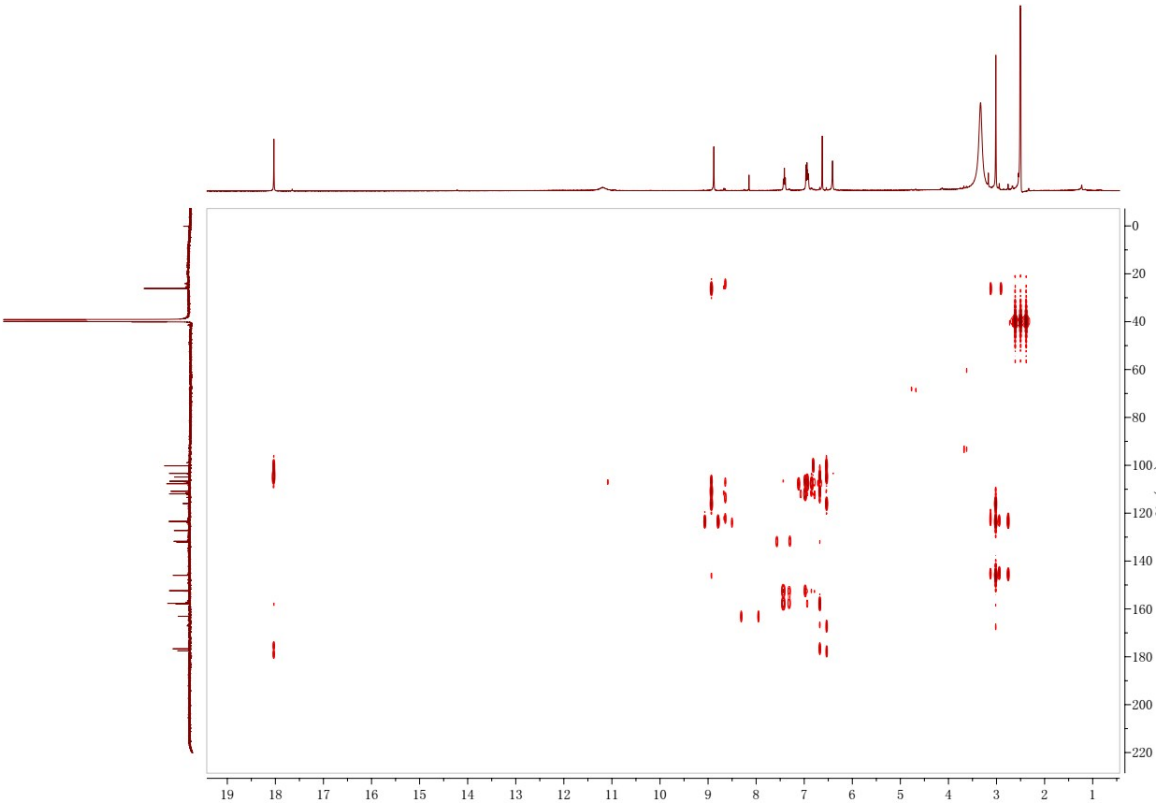

Fig. S65 HMBC spectrum of **20b** (DMSO-d_6)

Supplementary References

1 E. Szewczyk, T. Nayak, C. E. Oakley, H. Edgerton, Y. Xiong, N. Taheri-Talesh, S. A. Osmani, B. R. Oakley, *Nat. protoc.* 2006, **1**, 3111–3120.

2 H. Kikuchi, S. Ishiko, K. Nakamura, Y. Kubohara, Y. Oshima, *Tetrahedron* 2010, **66**, 6000–6007.

3 G. Tanabe, N. Tsutsui, K. Shibatani, S. Marumoto, F. Ishikawa, K. Ninomiya, O. Muraoka, T. Morikawa, *Tetrahedron* 2017, **73**, 4481–4486.

4 L. Zou, Z. X. Zhang, X. W. Chen, H. Chen, Y. Zhang, J. Q. Li, Y. Liu, *Tetrahedron* 2018, **74**, 2376–2382.